CENTRAL RESEARCH LIBRARY
DOCUMENT COLLECTION

MARTIN MARIETTA ENERGY SYSTEMS LIBRARIES
3 4456 0353140 8

ORNL 1343
Chemistry-Separation Processes
for Plutonium and Uranium 8a

LABORATORY RECORDS
1954

PROGRESS REPORT

PUREX PROCESS LABORATORY DEVELOPMENT

FEBRUARY THROUGH APRIL 1952

Classification Cancelled
Or Changed To
By Authority Of UCC 9-13-71
By C. Goodlett Date 11-10-71

AEC RESEARCH AND DEVELOPMENT REPORT

OAK RIDGE NATIONAL LABORATORY
OPERATED BY
CARBIDE AND CARBON CHEMICALS COMPANY
A DIVISION OF UNION CARBIDE AND CARBON CORPORATION
UCC
POST OFFICE BOX P
OAK RIDGE, TENNESSEE

SE[redacted]

Report Number ORNL-1343

This document consists of 71 pages. No. 8 of 136 copies. Series A.

Contract No. W-7405, eng 26

CHEMICAL TECHNOLOGY DIVISION

Laboratory Section

PROGRESS REPORT: PUREX PROCESS LABORATORY DEVELOPMENT, FEBRUARY THROUGH APRIL, 1952

J. R. Flanary
S. V. Castner
R. L. Folger
L. E. Line, Jr.
V. J. Reilly
V. A. Ryan
E. B. Sheldon

DATE ISSUED:

[redacted]

OAK RIDGE NATIONAL LABORATORY
Operated by
CARBIDE AND CARBON CHEMICALS COMPANY
A Division of Union Carbide and Carbon Corporation
Post Office Box P
Oak Ridge, Tennessee

MARTIN MARIETTA ENERGY SYSTEMS LIBRARIES

3 4456 0353140 8

[redacted]

ORNL 1343
Chemistry-Separation Processes
for Plutonium and Uranium

INTERNAL DISTRIBUTION

1. G. T. Felbeck (C&CCC)
2-3. Chemistry Library
4. Physics Library
5. Biology Library
6. Health Physics Library
7. Metallurgy Library
8-9. Training School Library
10. Reactor Experimental Engineering Library
11-14. Central Files
15. C. E. Center
16. C. E. Larson
17. W. B. Humes (K-25)
18. L. B. Emlet (Y-12)
19. A. M. Weinberg
20. E. H. Taylor
21. E. D. Shipley
22-23. F. L. Steahly
24. F. C. VonderLage
25. R. C. Briant
26. J. A. Swartout
27. S. C. Lind
28. A. H. Snell
29. A. Hollaender
30. M. T. Kelley
31. K. Z. Morgan
32. J. S. Felton
33. A. S. Householder
34. C. S. Harrill
35. C. E. Winters
36. D. W. Cardwell
37. E. M. King
38. W. K. Eister
39. F. R. Bruce
40. F. L. Culler
41. J. O. Davis
42. H. K. Jackson
43. D. D. Cowen
44. J. R. Flanary
45. S. V. Castner
46. R. L. Folger
47. L. E. Line, Jr.
48. V. J. Reilly
49. V. A. Ryan
50. E. B. Sheldon

EXTERNAL DISTRIBUTION

51-58. Argonne National Laboratory
59. Armed Forces Special Weapons Project (Sandia)
60. Armed Forces Special Weapons Project (Washington)
61-67. Atomic Energy Commission, Washington
68-70. Brookhaven National Laboratory
71-72. California Research and Development Company
73. Carbide and Carbon Chemicals Company (C-31 Plant)
74-75. Carbide and Carbon Chemicals Company (K-25 Plant)
76-77. Carbide and Carbon Chemicals Company (Y-12 Area)
78. Chicago Patent Group
79-84. duPont Company
85-88. General Electric Company, Richland
89. Hanford Operations Office
90-93. Idaho Operations Office
94. Iowa State College
95-98. Knolls Atomic Power Laboratory
99-101. Los Alamos
102. Massachusetts Institute of Technology (Benedict)
103-105. Mound Laboratory
106. Naval Research Laboratory
107-110. New York Operations Office
111-112. North American Aviation, Inc.
113. Patent Branch, Washington
114. Savannah River Operations Office (Augusta)
115. Savannah River Operations Office (Wilmington)
116-119. University of California Radiation Laboratory
120-121. Vitro Corporation of America
122-136. Technical Information Service, Oak Ridge

[redacted]

[redacted]

TABLE OF CONTENTS

		Page
1.0	Abstract	7
2.0	Introduction	8
3.0	Summary	8
4.0	Acknowledgements	11
5.0	Second Uranium Cycle Studies	12
5.1	Ruthenium Decontamination with Flowsheets Nos. 1 and 3	12
5.2	Effect of Feed Pretreatment on Decontamination	12
5.3	Miscellaneous Decontamination Studies	13
5.4	Near-Saturation Flowsheet	13
6.0	Uranium Product Tail End Treatment	16
6.1	Adsorption Studies with Unfiltered Solutions	16
6.11	Activity Removal by Filtration through Silica Gel	16
6.12	The Effect of Feed Composition and Type of Silica Gel on Zirconium -Niobium Adsorption	16
6.2	Adsorption Studies Using Filtered IEU Concentrate	18
6.21	The Effect of Flow Rate and Bed Depth on Decontamination and Capacity	18
6.22	The Effect of Temperature, Acidity, Feed Composition and Type of Silica Gel on Adsorption Efficiency	22
6.3	Silica Gel Bed Regeneration	26
7.0	Plutonium Recovery from Metallurgical Wastes	26
7.1	Slag and Crucible Dissolution	27
7.11	Iodine Removal	29
7.12	Silica Removal	29
7.13	Loss of Nitric Acid	34
7.14	Feed Adjustment	37
7.15	Feed Clarification	37
7.2	Solvent Extraction	38
7.21	Feed Preparation	38
7.22	Extraction and Stripping	42
7.23	Settling Time	42
7.24	Product Purity	44

[redacted]

TABLE OF CONTENTS (Cont'd)

		Page
	7.3 Product Concentration by Ion Exchange	46
	7.4 Corrosion Studies	46
	7.41 Survey Tests	46
	7.42 Durability Tests	47
8.0	Denitration of the Uranium Product	49
	8.1 Foaming Studies	49
	8.2 Ruthenium Behavior	49
9.0	Chemical Stability of Solvent Diluent	50
10.0	Nitrous Acid Behavior during Solvent Extraction	51
	10.1 Extraction of Nitrous Acid	51
	10.11 Instability of Nitrous Acid	51
	10.12 Determination of Distribution Coefficient	53
	10.2 Stripping of Nitrous Acid from the Solvent	56
11.0	Fumeless Dissolving	57
	11.1 Material Balance of the Reaction between K_2O_4 and NaOH	57
	11.2 Scrubbing of N_2O_4 with KOH	58
	11.3 Scrubbing of NO with HNO_3	58
12.0	The ORNL "mini" Mixer-Settler	59
13.0	Bibliography	63
14.0	Appendix	65

LIST OF FIGURES

Figure	Title	Page
6.1	The Influence of Flowrate on Zirconium and Niobium Adsorption from Uranyl Nitrate Solutions by Silica Gel	19
6.2	The Influence of Bed Depth on Zirconium and Niobium Adsorption from Uranyl Nitrate Solutinns by Silica Gel -- 3 cm/min Flowrate	20
6.3	The Influence of Bed Depth on Zirconium and Niobium Adsorption from Uranyl Nitrate Solutions by Silica Gel -- 1 cm/min Flowrate	21
6.4	The Effect of Flowrate and Bed Depth on Silica Gel Bed Capacity for Niobium	23
6.5	The Effect of Flowrate and Bed Depth on Silica Gel Bed Capacity for Zirconium	24
6.6	The Effect of Temperature on Zirconium and Niobium Adsorption from Uranyl Nitrate Solutions by Silica Gel	25
7.11	Slag and Crucible Dissolution Equipment	28
7.12	Temperature Variation and Fluoride Reaction Time during the Dissolution Cycle: Run DG 2	30
7.13	Temperature Variation and Fluoride Reaction Time during the Dissolution Cycle: Run DG 3	31
7.14	Temperature Variation and Fluoride Reaction Time during the Dissolution Cycle: Run DG 4	32
7.21	Batch Countercurrent Apparatus for Solvent Extraction	39
7.22	Extraction Conditions - Slag and Crucible Solution	40
7.23	Stripping Conditions - Slag and Crucible Solution	40
10.1	Nitrous Acid Distribution between Purex Solvent Mixture and Nitric Acid of Various Concentrations	55
12.1	The ORNL "Mini" Mixer-Settler	60
12.2	Mixer-Settler Feed Assembly	61
12.3	Stage Data for Uranium Extraction-Purex 1A Operation	62

LIST OF TABLES

Table	Title	Page
5.1	Effect of Feed Pretreatment on Second Uranium Cycle Decontamination	15
6.1	Zirconium and Niobium Adsorption from Unfiltered Uranyl Nitrate Solutions by Silica Gel	17
7.11	Dissolution Procedure Variables	33
7.12	Dissolution Residues	34
7.13	Theoretical Nitric Acid Requirements for Dissolution	35
7.14	Nitric Acid Material Balance for Dissolution	36
7.15	Solvent Extraction Feed Preparation	38
7.21	Composition of Feed Solutions for Batch Countercurrent Extractions	41
7.22	Summary of Batch Countercurrent Extraction Results	43
7.23	Time Required for Complete Phase Separation in Batch Countercurrent Extraction of Slag and Crucible Solution	44
7.24	Analysis of Product Solutions	45
7.25	Comparison of Plutonium Product Purity with Purex TBP	46
7.41	Survey Corrosion Tests of Various Materials	48
7.42	Duration Tests of Stainless Steel Type 309 Cb	48
10.1	Decomposition of 0.01 M Nitrous Acid under Various Conditions	52
10.2	Nitrous Acid Extraction by Amsco, TBP, and 30% TBP in Amsco	53
10.3	Nitrous Acid Extraction by 30% TBP in Amsco	54
10.4	Nitrous Acid Stripping from TBP with 1 M Nitric Acid	56
11.1	N_2O_4 Generated by Decomposition of $Pb(NO_3)_2$	57
11.2	Scrubbing of N_2O_4 by 20% KOH	58

1.0 Abstract

This report covers the Purex Process laboratory studies carried out during the past quarter: February through April, 1952. The results of work concerned with main line process refinements, plutonium recovery from metallurgical wastes, and problems evolving from the Purex Pilot Plant operation are discussed.

2.0 Introduction

During the past quarter Purex laboratory studies have been concerned primarily with process modifications which will permit all product specifications to be met with continuous two-cycle solvent extraction of Hanford production metal. Emphasis has been placed on the development and refinement of processing techniques which are: (a) simple and relatively inexpensive and (b) adaptable to continuous operation. Aside from the problems associated with the main line process (irradiated metal to purified, concentrated plutonium and uranyl nitrate solutions) the laboratory program also includes the development and small scale demonstration of plutonium recovery from metallurgical wastes, assistance to the Purex Pilot Plant group, and special studies not related to the ORNL-Purex mode of operation.

Although the first cycle and second plutonium cycle (ORNL Flowsheet #3) have been successfully pilot-planted, second uranium cycle decontamination is not quite adequate to consistently yield specification uranyl nitrate. Initially, the product was found to be too high in gamma activity, due almost entirely to the presence of excessive amounts of zirconium and niobium. At present, adequate removal of these contaminants from the concentrated uranium product is accomplished by adsorption on a fixed bed packed with silica gel.

More recently, excessive ruthenium has appeared in the uranium product from the first series of continuous pilot plant runs. This situation has prompted a search for methods of improving ruthenium decontamination which do not entail major process changes.

Other problems which have received attention this quarter include: fumeless dissolving, chemical stability of Purex diluent, solvent extraction of nitrous acid, and the ORNL "Mini" mixer-settler operation.

3.0 Summary

Laboratory investigation of methods designed to enhance the second cycle uranium-fission product separation has yielded promising results which, if reproducible in large scale equipment, should enable uranium trioxide specifications to be met without a head-end treatment or a third solvent extraction cycle. A process for plutonium recovery from metallurgical wastes, which includes dissolution, filtration, one-cycle solvent extraction, and ion exchange coupling, has been successfully demonstrated in batch, semiworks scale equipment with Los Alamos waste. In addition, effort has been devoted to diverse problems associated with fumeless dissolving, chemical stability of Purex diluent, solvent extraction of nitrous acid, and the ORNL "Mini" mixer-settler.

3.1 Fumeless Dissolving

A method[1] of N_2O_4 analysis of dissolver off-gases has been proposed which involves absorption of nitrogen tetroxide in sodium hydroxide according to the equation:

$$N_2O_4 + 2NaOH \longrightarrow NaNO_2 + NaNO_3 + H_2O$$

[redacted]

and colorimetric nitrite determination with Greiss reagent. It had been reported that under certain conditions N_2O_4 may not react quantitatively with alkali to give equimolar quantities of nitrite and nitrate. The method has been tested with accurately known concentrations of N_2O_4, which was found to be completely absorbed by 15% sodium hydroxide.

In cooperation with the Unit Operations Section, gas samples taken before and after scrubbing in a tower with 20% KOH were analyzed for nitrite. The results indicated 99% removal of N_2O_4 for two of the three runs made.

3.2 Chemical Stability of Purex Diluent

Upon request of the du Pont Company,[2] the chemical stability of Amsco 123-15 under the ORNL Purex Flowsheet #3 conditions is being examined. It is generally known that tributyl phosphate cut with a kerosene type diluent assumes a permanent yellow coloration when contacted with Purex aqueous streams. Controlled tests have established that the color is imparted to the diluent alone - and is associated with the HNO_3-HNO_2 system. The yellow color probably results from limited nitration (and possibly oxidation) of unsaturates contained in the diluent. Earlier work[3] had shown that continuous room temperature contact of 30% TBP in Amsco with 6 M HNO_3 for 17 days resulted in 0.02% fixed nitrogen in the organic phase.

3.3 TBP Extraction of Nitrous Acid

Purex solvent mixture was found to possess a high affinity for nitrous acid, due almost entirely to TBP. Nitrous acid distribution between 30% TBP in Amsco and 0.01 M HNO_2 in 0, 1, and 6 M HNO_3 was found to be 15, 20, and 3, respectively. Stripping of the nitrous acid from the organic with 1 M HNO_3 was extremely difficult; 27 washes were required to effect 90% removal.

3.4 The ORNL "mini" Mixer-Settler

Repeated difficulties have been encountered during construction and testing of the laboratory mixer-settler, the majority of which have been corrected except for occasional leakage out the bottom of the fluorothene block. Three inactive 1A runs, per Purex ORNL Flowsheet #1, have been completed in the 20 stage unit with generally satisfactory results. End stream and stage data from an 18 hour run indicated that steady state was reached after 15 hours operation (five aqueous throughputs). Uranium extraction stage efficiency averaged 90%, omitting the last stage whose efficiency was unaccountably low (7.9%). Uranium loss through six stages was 0.002%.

3.5 Modified Second Uranium Cycle

Coincident with the introduction of continuous two-cycle operation at the Pilot Plant, excessive ruthenium has appeared in the Purex uranium product. Since the silica gel tail end treatment does not remove ruthenium, other means were sought to improve ruthenium decontamination via the second solvent extraction cycle.

Batch countercurrent studies have shown that ORNL Flowsheet #1 is superior to Flowsheet #3 with respect to ruthenium decontamination.

The addition of 0.05 M sodium nitrite to the 1DF, followed by heating, increases the ruthenium separation by a factor of four to ten. Similar treatment with urea was nearly as effective as nitrite.

Operation with a near-saturation flowsheet, substitution of sodium nitrate for nitric acid in the scrub (i.e., high pH scrub), and the addition of a two-stage solvent scrub section to the stripping bank were tested. No improvement in ruthenium decontamination was observed.

3.6 Uranium Product Tail End Treatment

Study of the variables thought to influence zirconium-niobium adsorption on silica gel has continued using 1EU concentrate from recent pilot plant continuous runs as feed. Major emphasis was placed on the effect of bed depth and flowrates; however, other variables such as temperature, acidity, type of silica gel, and feed composition received attention.

It was noted that silica gel functions as a filter for suspended matter which carries roughly two-thirds of the gamma activity present. Consequently, filtered feeds were used to obtain data which could be interpreted on the basis of decontamination by adsorption alone.

At superficial linear velocities of 1 cm/min or less through a 20 cm by 1 sq. cm bed, or at a 3 cm/min rate with bed depths of 40 cm or more, a capacity of 200 - 250 ml of uranium product per ml of bed was realized with decontamination factors of 15 for niobium and 4 for zirconium. If less decontamination is required, the bed capacity will be significantly larger.

Adsorption at 70°C instead of room temperature appears to increase the zirconium-niobium decontamination or bed capacity two fold.

In this application, Davison refrigeration grade silica gel was found to be equal or superior to a sample supplied by Davison on request for "activated" silica gel.

Small variations in feed composition (acidity, fission product concentration and distribution, etc.) have not shown any conclusive effect on zirconium-niobium adsorption.

3.7 Uranium Product Denitration

It had been previously observed that denitration of Pilot Plant uranium product was accompanied by excessive foaming, due to dibutyl acid phosphate formed from entrained solvent. Products, obtained from recent Pilot Plant runs employing an after separator, showed little or no foaming during laboratory denitration experiments.

Ruthenium distillation occurred when denitrations were carried to 90% completion in both all-glass and part-stainless steel laboratory equipment. Ruthenium decontamination factors varied from 4 to 13 in glass; whereas, in two experiments in glass-stainless steel, the decontamination factor was three. All of the ruthenium distilled appeared in the acid scrubber.

3.8 Plutonium Recovery from Metallurgical Wastes

A dissolution procedure for slag and crucible wastes has been developed on a pilot scale which permits 99% plutonium recovery in a form (after filtration) suitable for direct solvent extraction with TBP.

Separation of plutonium from gross impurities (Al, Ca, Mg) is accomplished by one-cycle solvent extraction with 30% TBP - 70% Amsco solvent under conditions similar to the Purex second plutonium cycle (ORNL Flowsheet #3). The aqueous product is further decontaminated and concentrated by ion exchange coupling, prior to peroxide precipitation.

Approximately 115 liters of slag and crucible solution have been processed through batch countercurrent equipment. Plutonium extraction and stripping losses averaged 0.06 and 0.03%, respectively. Spectroscopic analyses show that calcium is the principal product contaminant. The product purity, however, is comparable to that of 2BP from the ORNL Pilot Plant Purex Run HP-13. Approximately 10 grams of recovered plutonium will be isolated by ion exchange and shipped to Los Alamos for evaluation.

Studies are underway to determine the most suitable construction material for the metallurgical waste dissolution equipment from the standpoint of availability, ease of fabrication, and resistance to attack by the corroding medium (nitric acid, hydrofluoric acid, and iodine). Based on survey corrosion tests of several stainless steels and Pfaulder glass, stainless steel type 309 Cb was chosen for further investigation.

Durability tests of unwelded, welded, and welded-pickled 309 Cb samples are 50% completed (five 24 hour corrosion cycles). The welded-pickled samples exhibited least corrosion: 0.027, 0.018, and 0.014 inches per year in vapor, liquid, and interface, respectively.

4.0 Acknowledgements

The assistance of the following ORNL personnel is greatly appreciated: C. L. Burros, L. T. Corbin, J. H. Edgerton, G. R. Wilson and E. I. Wyatt for analytical assistance; and A. W. Clark and A. M. Tripp for design and procurement of special equipment. The authors also wish to acknowledge the contributions of other sites: Los Alamos and Hanford for suggestions relative to slag and crucible dissolution and KAPL for mixer-settler design data.

5.0 Second Uranium Cycle Studies (V. J. Reilly, L. A. Byrd)

5.1 Ruthenium Decontamination with Flowsheet Nos. 1 and 3

In the two-cycle Purex Process with uranium tail end treatment, the uranium decontamination appears to be limited by ruthenium. A comparison of Pilot Plant results (Runs HP 8, 9, and 13) indicates that better ruthenium decontamination was obtained in the Purex No. 1 flowsheet than in the No. 3 flowsheet. These flowsheets were compared in the laboratory using feed prepared from Pilot Plant first cycle product. The ruthenium DF was 82 for Flowsheet No. 1 and about 40 for Flowsheet 3 at 85% uranium saturation. Although ruthenium decontamination was relatively low in all the runs it appeared that flowsheet No. 1 was more satisfactory.

5.2 Effect of Feed Pretreatment on Decontamination

In view of the poor ruthenium decontamination experienced during the flowsheet comparison studies, other methods were sought to increase the uranium-ruthenium separation via the second solvent extraction cycle. The following feed pretreatments have been found of some value: reflux with sodium nitrite, reflux with nitric acid, reflux with urea, and simmer at 85° C with either nitrite or urea. These treatments have been applied to both first cycle product concentrate (1CU boildown) and second cycle feed (1DF) from recent Pilot Plant runs, at acidities ranging from 0.5 to 2 M in nitric acid. The treatments were evaluated by processing the treated feed through batch countercurrent extraction, scrub and strip simulating 1D and 1E column operation. Purex No. 1 flowsheet, modified to provide 90% uranium saturation at the feed plate, was used. The results are given in Table 5.1.

A comparison of the gross gamma and ruthenium decontamination data from runs carried out on a single batch of 1CU concentrate indicates the beneficial effect of reflux or simmer with 0.05 M sodium nitrite, and to somewhat lesser extent, of heating with urea. Results from runs made with HCP 4 feed are obscured by the relatively high ruthenium decontamination when no treatment was employed. On the basis of these experiments, the maximum ruthenium separation is obtained when the feed is made 0.05 M in sodium nitrite and either refluxed for one hour or simmered at 85°C for three hours.

There is a disadvantage in the use of $NaNO_2$ in feed pretreatment since, if appreciable nitrite remains after digestion, it will be incompatible with ferrous sulfamate in a pulse column. This incompatibility is due to the reaction between the two with the generation of gaseous nitrogen. (The ferrous sulfamate is added to the 1D column scrub solution to reduce trace plutonium to the trivalent state in order to obtain final separation from the uranium product). Since nitrous acid is relatively unstable in the presence of air (see section 10.11), residual nitrite may be destroyed by air-sparging the treated feed prior to solvent extraction. This scheme will be tested in the laboratory.

The differences from batch to batch are apparent from the data in Table 5.1. It is seen that the product from HCP 4 is much easier to decontaminate from ruthenium than those from HCP 3 or 5. Performance with HCP 3 and 5 products was quite comparable to that experienced with HCP 2 product (flowsheet comparison runs) and is believed at present to be more typical of what to expect from the ORNL pilot plant as regards behavior in the second uranium cycle.

Determination of the gross gamma and specific fission product decontamination factors is subject to appreciable error because of the low level of acitivity in the second cycle uranium product. For example, the gross gamma activity is only twice the ion-chamber background with a 50 ml sample when a DF of about 400 is obtained. Likewise, 100-140 c/m/ml of ruthenium beta is equivalent to the total fission product gamma activity tolerable in recovered uranium, which approaches the limit of detection of this contaminant by beta counting. In order to provide DF values for niobium and zirconium, these constituents were measured in the gamma scintillation counter. Even with the high counting efficiency gained by this method, the count was below the instruments background when good decontamination was experienced.

In the last four runs with HCP 5 product 0.05 M sulfuric acid was substituted for ferrous sulfamate in the scrub solution in an attempt to obtain final removal of residual plutonium by sulfate complexing. The plutonium DF varied from 6 to 80; whereas a DF of 30 to 50 is needed across the second uranium cycle to meet the ten parts per billion plutonium specification which applies to recovered uranium.

5.3 Miscellaneous Decontamination Studies

The effect of a high pH solution on ruthenium decontamination in the scrub section was examined in one run (Flowsheet #1 conditions) where 3 M sodium nitrate was substituted for 3 M nitric acid as scrubbing agent. The ruthenium decontamination factor across the second cycle was only 30 as compared to 76 obtained with the nitric acid scrub. It was thought that additional fission product-uranium separation might be achieved in the uranium strip contactor by addition of a solvent scrub section which would back extract residual activity from the aqueous product stream. One run was made with a two stage solvent scrub section coupled to the seven stage stripping bank. No improvement in gross gamma decontamination was detected. Further work with this arrangement is planned to study the behavior of individual fission products.

5.4 Near-Saturation Flowsheet

Further work on a near-saturation flowsheet was suspended when its instability to flow and composition variations developed. Previous work had indicated that maximum separation of uranium from fission products should be achieved with solvent extraction conditions adjusted such that nearly 100% uranium saturation of the solvent (TBP) is maintained. Such an arrangement would leave virtually no tributyl phosphate for complexing of fission products

which should permit more efficient separation.

Batch countercurrent studies of the most promising flowsheet, employing a 1.68 M uranium - 2 M nitric acid feed, a 30% TBP extractant, and a 0.5 M nitric acid scrub at a feed/extractant/scrub flow ratio of 20/78/10, has shown this system to be unsteady over long periods of operation. This was not immediately apparent since the change toward increased uranium in the extraction section was very slow. An analysis of the problem has led to the conclusion that a system based on salting by nitric acid whose concentration is obtained to a significant extent by reflux will not be stable to upset.

Any departure from flowsheet specifications which would put additional uranium into the extraction section will decrease the nitric acid salting strength by decreasing the acid reflux. Thus the upset would be self-perpetuating. Considering the conditions in the scrub section when a temporary increase in uranium feed (or decrease in solvent) occurs, in order for the system to remain stable a higher concentration of uranium in the organic product must be obtained. However, this means a closer approach to saturation in the scrub stages, and the uranium distribution coefficient decreases as saturation is approached. Therefore the system would be self-healing only if the degree of saturation is far enough removed from 100% to permit these fluctuations without reaching such a low uranium distribution coefficient that the excess uranium is not quickly removed in the organic product.

This discussion has assumed no control instrument on the contactor other than to maintain the feeds at the design level. However, if an instrument were available to regulate either feed rate or solvent rate to control uranium concentration (or specific gravity) midway in the extraction section, it appears perfectly feasible to operate the 1D contactor very close to saturation at the feed plate. Since such a control does not appear particularly difficult to design into a mixer-settler, the advantage of a near-saturation flowsheet will be kept in mind for future work.

Table 5.1

Effect of Feed Pretreatment on Second Uranium Cycle Decontamination

Conditions: Flowsheet #1, 90% uranium saturation at the feed plate.

Extraction: Feed: 1.47 M U - 2 M HNO_3 prepared from pilot plant first cycle product

Extractant: 30% TBP in Amsco 123-15

Scrub: 3 M HNO_3

F/X/S ratio of 30/100/20 ml

5 Extraction and 4 scrub stages

Strip: Extractant stripped with double volumes of demineralized water

7 stages

Feed Stock	Feed Treatment	Decontamination Factors	
		Gross γ	Ru
HCP-3	None	44	76
HCP-3	Adjusted feed refluxed 3 hours	106	90
HCP-3	Made 0.05 M in $NaNO_2$, let stand 1 hour at 25°C	184	90
HCP-3	Made 0.05 M in $NaNO_2$, refluxed 30 min.	260	290
HCP-4	None	190	230
HCP-4	Made 0.05 M in $NaNO_2$, let stand 8 hrs. at 25°C	460	150
HCP-4	Made 0.05 M in $NaNO_2$, refluxed 30 min.	430	300
HCP-5	None	160	50
HCP-5	Made 0.1 M in urea, simmered 3 hrs. at 85°C	430	100
HCP-5	Made 0.05 M in urea, simmered 3 hrs. at 85°C	400	155
HCP-5	Made 0.1 M in urea. refluxed 1 hour	435	290
HCP-5	Made 0.05 M in $NaNO_2$, refluxed 30 min.	560	500
HCP-5	Made 0.05 M in $NaNO_2$, simmered 3 hrs. at 85°C	450	800

6.0 Uranium Product Tail End Treatment (V. J. Reilly, L. A. Byrd)

Laboratory study of zirconium and niobium adsorption from the second uranium cycle product (IEU boildown) by silica gel was resumed this quarter when a fresh supply of feed from Purex Pilot Plant continuous runs became available. This treatment has been proposed[4] as a feasible means of separating uranium from residual zirconium and niobium, which have consistently limited the fission product gamma decontamination obtained by two solvent extraction cycles.

A total of twelve adsorption runs have been made in laboratory (glass) columns with conditions varied such that the effect of flowrate, bed depth, type of silica gel, feed composition, and temperature on decontamination and bed capacity could be studied. The results of this work are discussed in the sections which follow.

6.1 Adsorption Studies with Unfiltered Solutions

6.11 Activity Removal by Filtration through Silica Gel

The first series of runs in this program (6 through 10) was carried out on unfiltered IEU boildown. It was soon apparent that particulate matter in the feed was being filtered out on the bed, and that this matter carried a substantial proportion of the activity present. Partial correction was made for this effect during this period by obtaining radiochemical analyses for zirconium and niobium (see Appendix A) on filtered samples of feed and calculating the decontamination on this basis. This provides the decontamination factor for adsorption only (not including that due to filtration), if the silica gel bed removes all of the suspended matter and if exchange does not occur with activity adsorbed on the particles. However, after run 10 it was obvious that removal of suspended matter was necessary prior to passage through the bed if erratic results were to be avoided. The results of runs 6 through 10, given in Table 6.1, should not be given as much significance as later runs which were made with filtered feed. The former indicate, however, that compared to previous results[5] with 3 cm/min flow through a 20 cm by 1 sq cm bed, decontamination is less and capacity is considerably higher before a definite breakthrough occurs.

6.12 The Effect of Feed Composition and Type of Silica Gel on Zirconium-Niobium Adsorption

Comparison of run 7 with run 9 indicates (Table 6.1) the superiority of Davison refrigeration-grade gel over that used in run 7, which was supplied by Davison on request for "Activated" silica gel. It is seen that with "activated" gel, the zirconium and niobium removal is 25 and 50%, respectively, of that obtained with the refrigeration grade gel.

Table 6.1

Zirconium and Niobium Adsorption

from Unfiltered Uranyl Nitrate Solutions by Silica Gel

Conditions: Varied except for flow rate (3 cm/min) and temperature (25°C)

Run No.	Feed			Bed Size (cm x sq. cm)	Throughput (ml/ml of bed)	Instantaneous[1] Decontamination Factors	
	Source	U(M)	HNO_3(M)			Zr	Nb
6	IEU boildown	1.68	0.3	20 x 1	60 170 340	12 -- 20	3.4 4 4
7[2]	IEU boildown	1.68	0.41	20 x 1	200	1	2.7
8[3]	ICU boildown	1.76	0.52	24 x 0.25	170	1.2	3.4
9	IEU boildown	1.68	0.4	20 x 1	50 200	6 4	5.7 5.0
10	IEU boildown	1.68	0.9	20 x 1	100 300 460	2 -- 2	3.2 3 3

(1) DF by adsorption only. Inclusion of filtration DF would increase these values roughly three-fold.

(2) Davison "activated" silica gel.

(3) Silica gel is -40 +60 mesh.

The zirconium behavior in Run 8, wherein ICU concentrate was used, may be due to the presence of more than one kind of zirconium in the system. A small diameter bed (0.25 sq cm cross section) packed with -40 +60 mesh silica gel was used in this run in order to operate with a minimum volume of first cycle product and cut down the radiation background.

There is evidence of a trend toward decreased zirconium removal with increase in feed acidity (runs 6, 9, and 10). Nevertheless, it is felt that the influence of feed acidity on overall decontamination is slight, particularly in the range of 0.3 to 0.9 M nitric acid covered in this work.

6.2 Adsorption Studies using Filtered IEU Concentrate

6.21 The Effect of Flow Rate and Bed Depth on Decontamination and Capacity

Feed for succeeding runs (12 through 17) was prepared by combining IEU concentrate from two (high level) Pilot Plant runs and passing this through a plug of pyrex glass wool one inch in diameter by two inches thick. The filtrate appeared to be perfectly clear, and contained 35 mv γ activity/ml as compared with 109 mv/ml for the unfiltered solution (Bldg. 3550 ion chamber). As successive samples of the filtrate showed no trend toward increased activity with increased volume throughput, this reduction in activity is not likely to be due, to any extent, to adsorption on the glass fibers.

Four runs (12, 13, 14, and 17) have been made with this feed to determine the effect of flow rate and bed depth on decontamination and capacity. The results of these runs (decontamination by adsorption only) are plotted in Figures 6.1, 6.2, and 6.3. Figure 6.1 illustrates the effect of decreased flowrate through a 40 cm bed on zirconium-niobium decontamination. It is noted that at 3 cm/min flowrate (Run 13) the instantaneous DF for niobium averages 11.6 across the plateau region of the curve. Decrease in flowrate to 1 cm/min (Run 17) raises the DF to 15. Similarly, the zirconium DF is increased from 3.5 to 5.

The same behavior is apparent in Figures 6.2 and 6.3, which show a gain in zirconium-niobium decontamination when the bed depth is doubled and the flow rates maintained constant. It is seen that the niobium decontamination factor ranges from 3 (Run 12, 3 cm/min flow through a 20 cm bed) to 15 (Run 17, 1 cm/min flow through a 40 cm bed). The corresponding values for zirconium are 2 and 5 for runs 12 and 17, respectively.

Run 12 was conducted at the same feed rate and bed depth as runs 6 through 10, and the results are roughly equivalent (except for Zr behavior in Runs 6 and 8). It is immediately obvious that the conditions for Run 12 (3 cm/min flow through a 20 cm bed) are inadequate to derive the most good from the silica gel bed. Increasing the sojourn time by doubling the bed depth or by decreasing to a third the flow rate markedly increases the DF.

Figure 6.1

The Influence of Flowrate on
Zirconium and Niobium Absorption from Uranyl Nitrate Solutions by Silica Gel

Conditions: Feed - Filtered IEU Boildown (1.68 *M* U - 0.94 *M* HNO_3)
Silica gel - Davison (refrigeration grade), -20 + 40 mesh
Bed size - 1 sq cm by 40 cm
Flowrate - 1 cm/min (Run 17)
3 cm/min (Run 13)

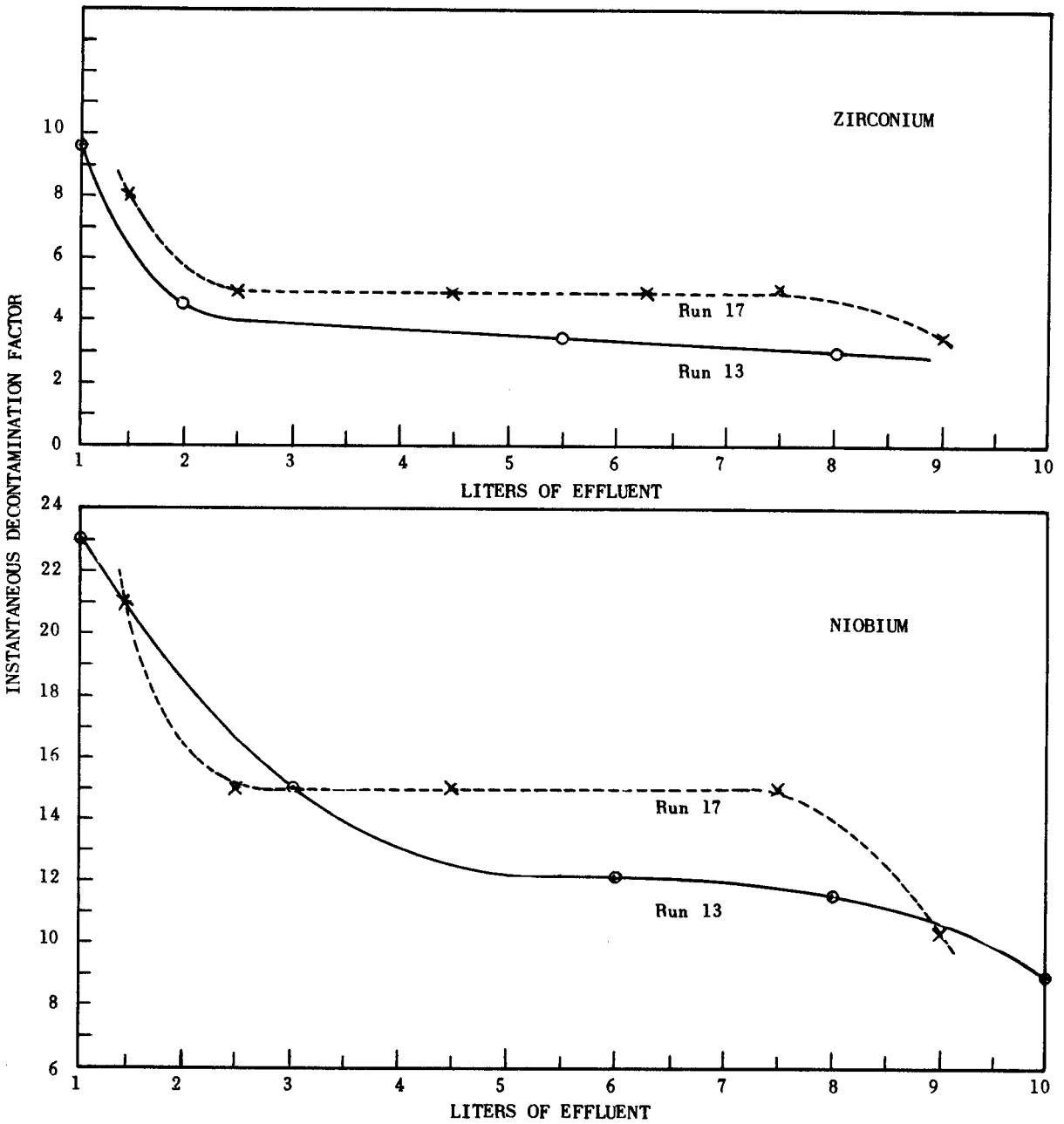

Figure 6.2

[redacted]
DWG. 15696

The Influence of Bed Depth on
Zirconium and Niobium Adsorption from Uranyl Nitrate Solutions by Silica Gel
3 cm/min Flowrate

Conditions: Feed - Filtered IEU Boildown(1.68 *M* U - 0.94 *M* HNO_3)
Silica gel - Davison (refrigeration grade), - 20 + 40 mesh
Flowrate - 3 cm/min
Bed size - 1 sq cm by 20 cm (Run 12)
1 sq cm by 40 cm (Run 13)

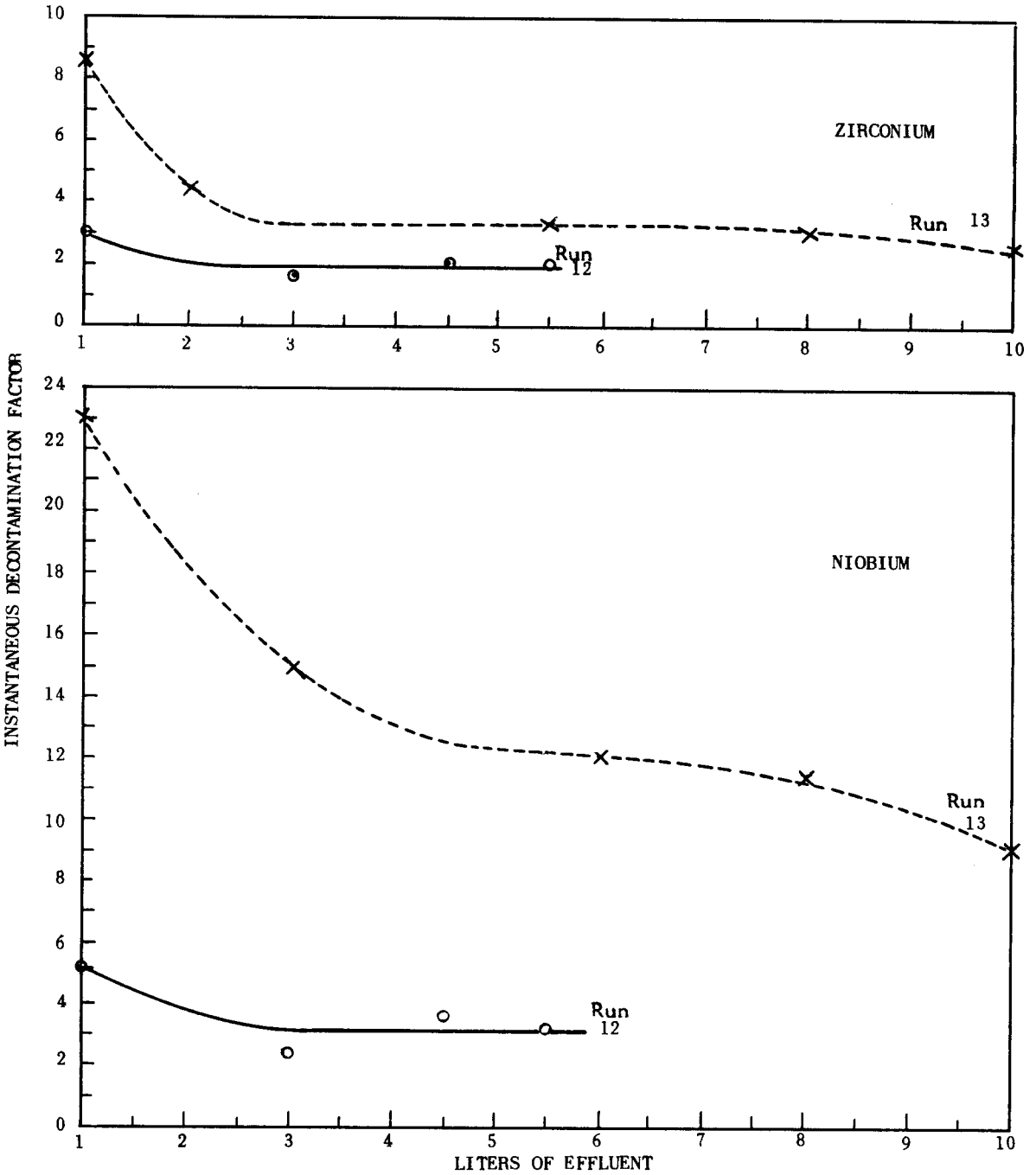

Figure 6.3

[redacted] DWG. 15697

The Influence of Bed Depth on
Zirconium and Niobium Adsorption From Uranyl Nitrate Solutions by Silica Gel
1 cm/min Flowrate

Conditions: Feed - Filtered IEU Boildown (1.68 *M* U - 0.94 *M* HNO_3)
Silica Gel - Davison (refrigeration grade), - 20 + 40 mesh
Flow rate - 1 cm/min
Bed size - 1 sq cm by 20 cm (Run 14)
1 sq cm by 40 cm (Run 17)

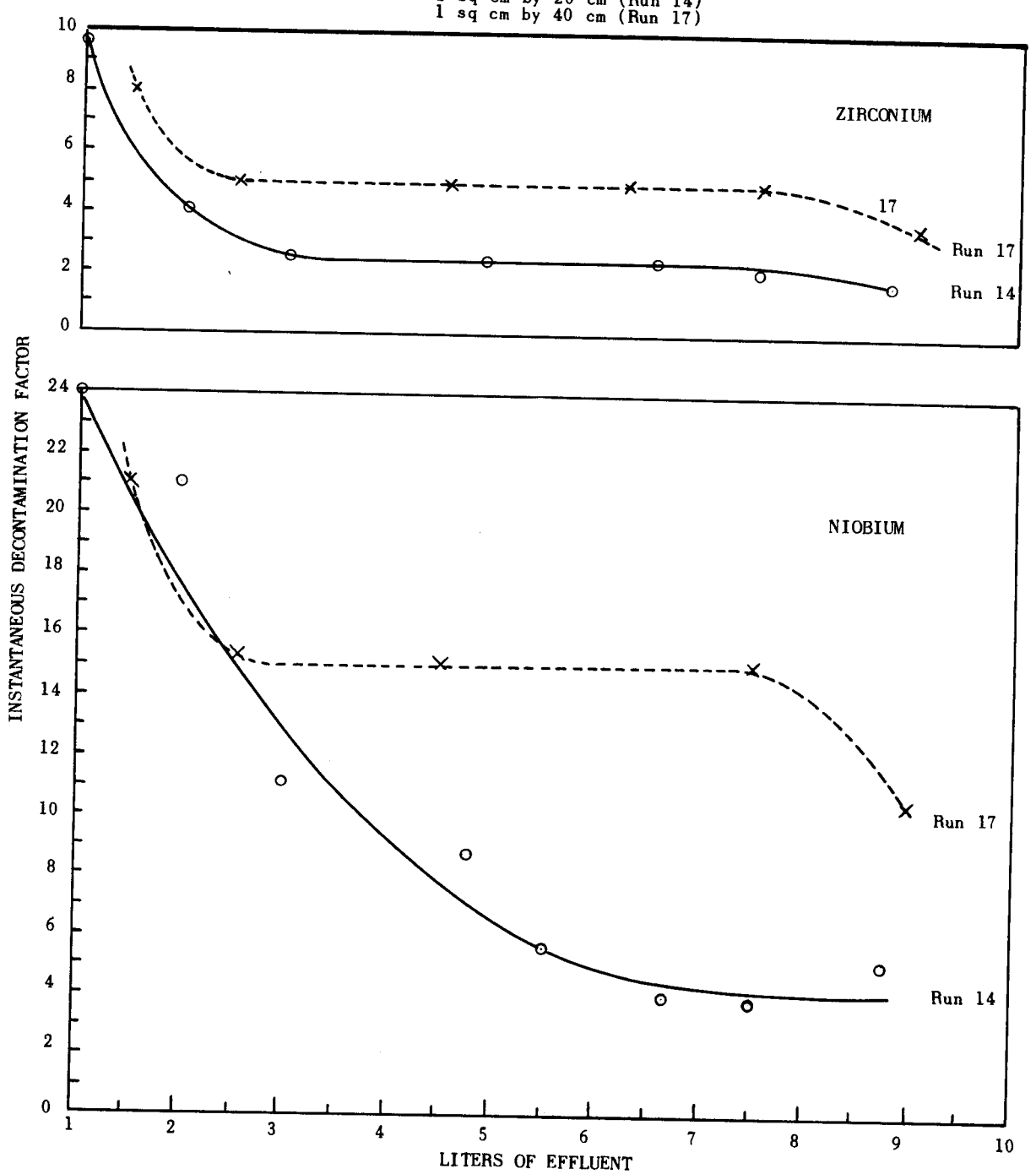

In order to apply these results to the practical problem of decontaminating uranium product to a satisfactory level, they have been replotted in Figures 6.4 and 6.5 where now the DF is the integrated value for the composite effluent (see Appendix B for integration method used). To use these plots, one first decides what overall niobium or zirconium decontamination factor is needed. Then, off the plot is read the volume of solution which may be treated under the specified conditions of bed depth and superficial flow rate before this overall DF is reached. This is the capacity of the bed under these conditions. As an example, if the feed activity is such as to require a niobium DF of 15 and zirconium DF of 4 by adsorption, the capacity would be, for the various cases:

Flow Rate (cm/min)	Bed Depth, (cm)	Capacity - Nb (ml of effluent/ml of bed)	Capacity - Zr (ml of effluent/ml of bed)
3	20	0	50
3	40	190	225
1	20	215	200
1	40	240	320

The similarity of the curves for runs 13, 14, and 17 (Figures 6.4 and 6.5) indicates that limiting capacity is being approached under these conditions. Thus, a marked increase in unit capacity would not be expected if the flow rate were dropped below 1 cm/min or the bed length were increased beyond 40 cm with a flow rate of 3 cm/min. (An increase in bed length would probably be desirable for a plant-scale adsorber because of the channelling which occurs in large diameter equipment.

6.22 Effect of Temperature, Acidity, Feed Composition, and Type of Silica Gel on Adsorption Efficiency

The effect of temperature was investigated briefly in Runs 12 and 15. Run 12 was made at room temperature (about 30°C), whereas Run 15 was made at 70°C. The results of these runs are compared in Figure 6.6. At the rate (3 cm/min) and bed depth (20 cm) used, operation at 70°C increased decontamination by about a factor of two. Repetition of this study with longer sojourn time is planned.

A brief comparison of two runs at different acidities has been made (Runs 16 and 12). Here all conditions were the same except for the acidity, which was 0.45 N in Run 16, and 0.9 N in Run 12. Feed for Run 16 was adjusted to the lower acidity by mixing the filtered feed solution with an equal volume of filtered, neutral solution of the same uranium concentration. The radiochemical results were uncertain in Run 16, so the gross γ DF, corrected for ruthenium and UX, was calculated and was found to be roughly half that for Run 12. This result, however, does not check with the earlier work, shown in Table 6.1, where roughly the same results were obtained at acidities ranging from 0.3 to 0.9 N HNO_3. Further investigation of the effect of acidity may be indicated if the results at the normal acidity (0.9 N) are not completely satisfactory.

Figure 6.4

The Effect of Flowrate and Bed Depth on Silica Gel Bed Capacity for Niobium

Conditions: Feed - Filtered IEU Boildown (1.68 *M* U - 0.94 *M* HNO_3)
Silica gel - Davison (refrigeration grade), - 20 + 40 mesh
Bed cross section - 1 sq cm

Bed depth and flowrate -			
20 cm	- 3 cm/min	- Run	12
40	- 3		13
20	- 1		14
40	- 1		17

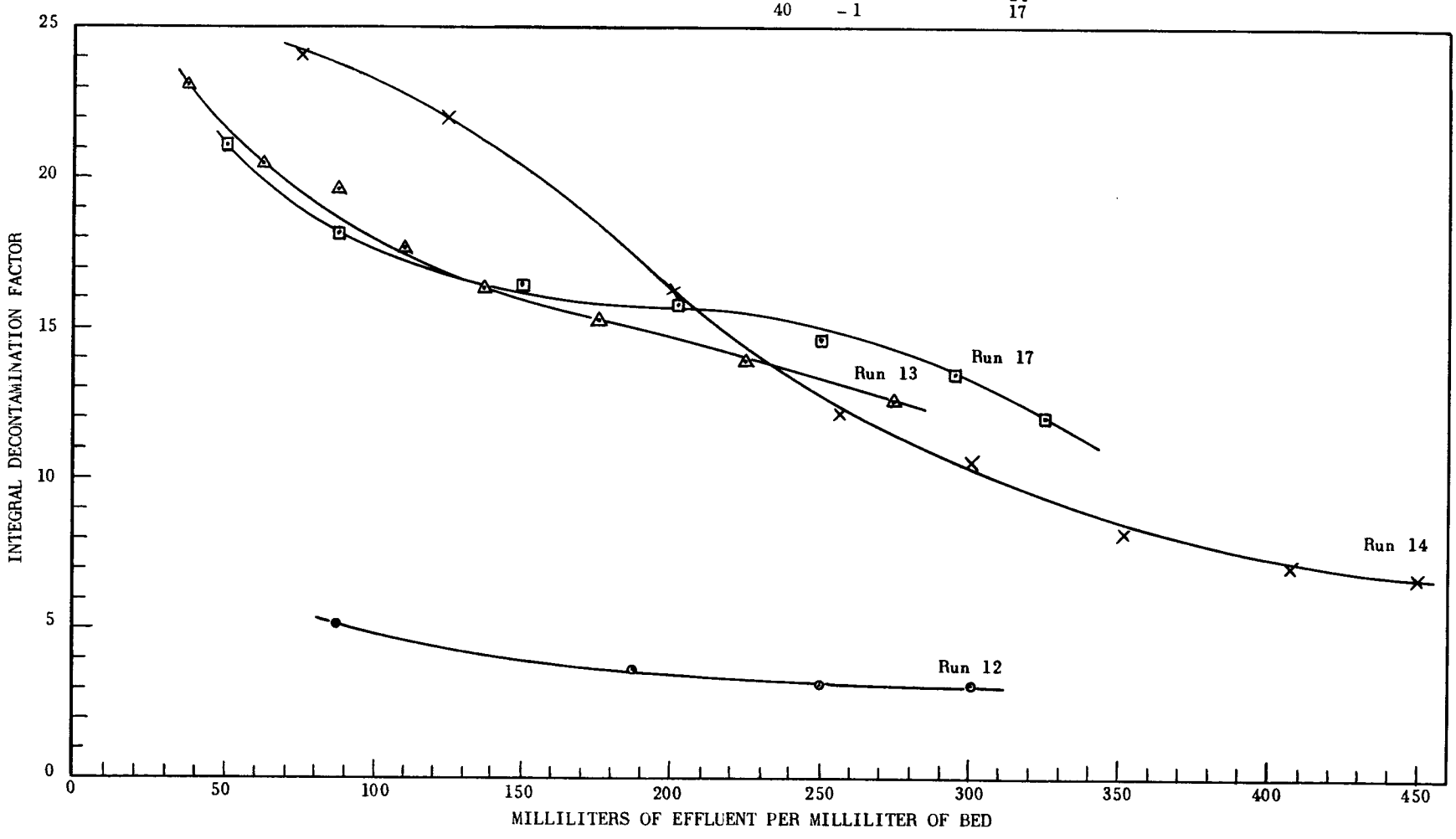

Figure 6.5

The Effect of Flowrate and Bed Depth on Silica Gel Bed Capacity for Zirconium

Conditions: Feed - Filtered IEU Boildown (1.68 *M* U - 0.94 *M* HNO_3)
Silica gel - Davison (refrigeration grade), - 20 + 40 mesh
Bed cross section - 1 sq cm

Bed depth	and flowrate		
20 cm	- 3 cm/min	-	Run 12
40	- 3	-	13
20	- 1	-	14
40	- 1	-	17

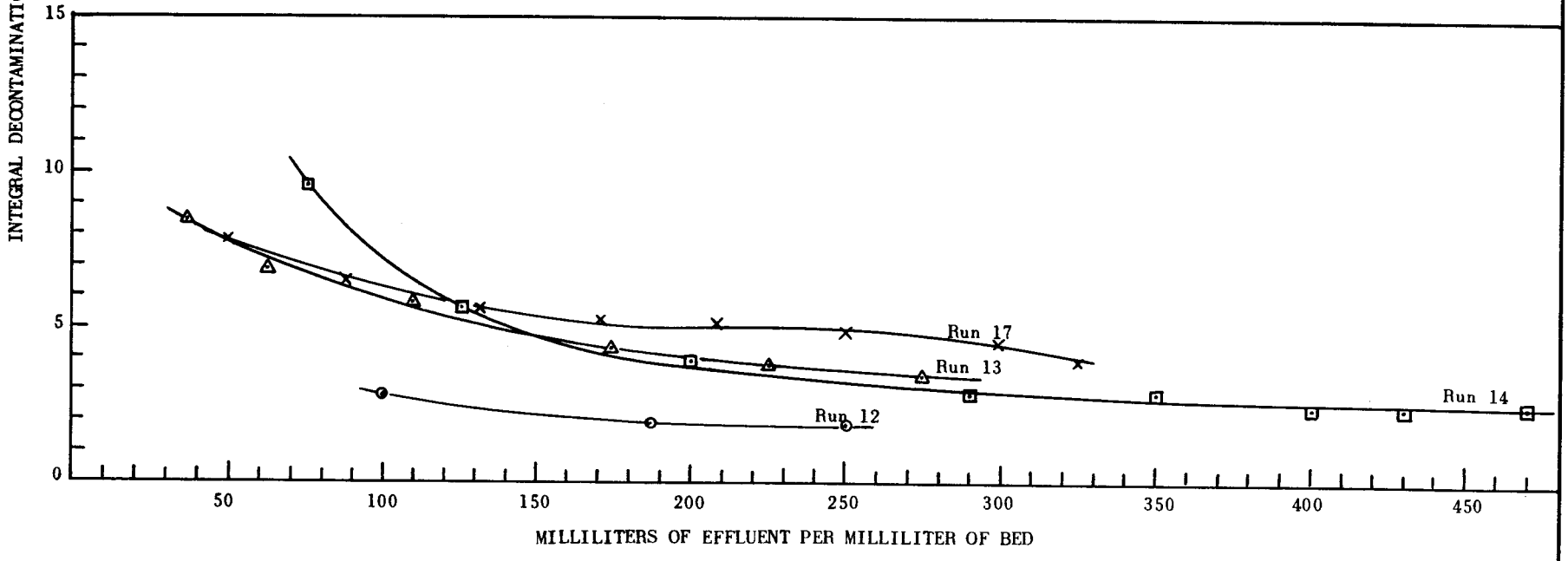

Figure 6.6

The Effect of Temperature on Zirconium and Niobium Adsorption from Uranyl Nitrate Solutions by Silica Gel

Conditions: Feed – Filtered IEU Boildown (1.68 *M* U – 0.94 *M* HNO_3)
Silica Gel – Davison (refrigeration grade) – 20 + 40 mesh
Bed Size – 1 sq cm by 20 cm
Flow rate – 3 cm/min

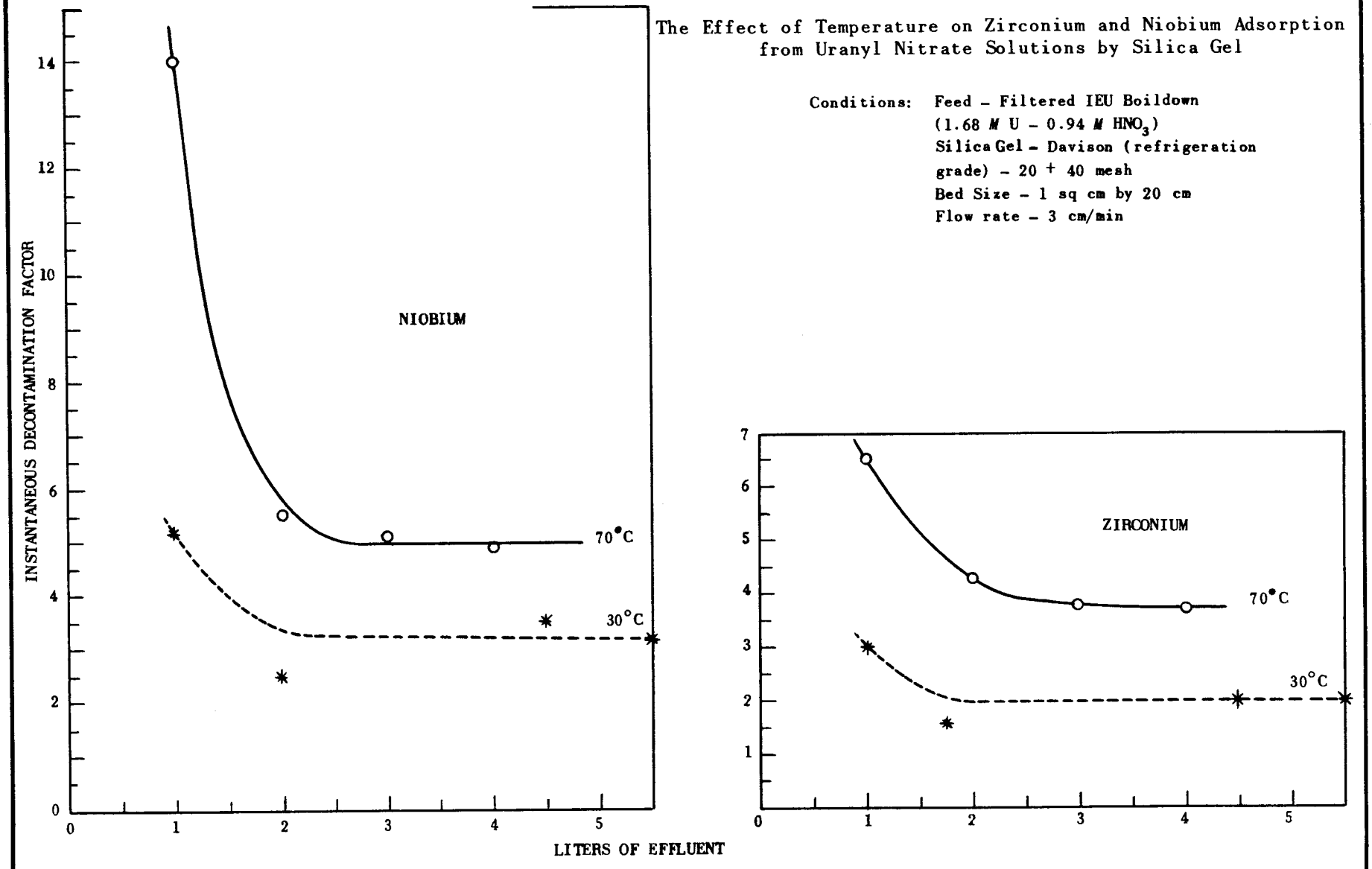

Since it is quite possible that more than one form of niobium and/or zirconium are present in the feed, each with its own behavior with silica gel, it will be necessary to repeat some of these experiments with other batches of IEU boildown as they become available to investigate this possibility. Some of the variations in the results reported here may be due to the presence of several forms of niobium and zirconium in differing proportions (cf. runs 6, 8, 10, and 12 with regard to Zr) as well as to the effect of particulate matter which was present in the earlier runs. The question of aging may also apply, to a lesser extent, to some of the results reported here, although there is no clear indication that behavior has changed with age. Runs 15, 16, and 17 were made after the feed had aged for from three to five weeks.

6.3 Silica Gel Bed Regeneration

When capacity is reached, the silica gel bed is reconditioned in the following manner. First, occluded uranium is washed from the bed with two to three volume changes of 0.5 M HNO_3, which in plant operation would be returned to recycle. Then the zirconium-niobium activity is eluted from the gel with 0.4 M oxalic acid at 70°C, and jetted to waste. Finally, the traces of oxalic acid are flushed out of the bed with water.

Continued study of the elution step has shown that 0.4 M oxalic acid at 70°C consistently removes 85-90% of the activity in the first two to three volume changes. The elution tails off, however, and after 10 volume changes the bed activity is not dropping rapidly. This should be of little consequence, as radiochemical analyses indicate the behavior of niobium and zirconium are roughly the same on elution, so that it should be sufficient to regenerate by removing 85-90% of the activity, leaving the remainder as a heel.

A total of eight runs have been made on one bed of silica gel, which was regenerated to roughly 95% completion after each run with 0.4 M oxalic acid at 70-80°C. This bed was used in Runs 6, 10, 12, and 15 reported here, and no effects noted in these runs are ascribed to the previous history of the bed. Runs 11, 13, and 17 were also made with one bed, reconditioned between runs as described above. Here also, there is no indication of detrimental effects due to previous use of the bed.

7.0 Plutonium Recovery from Metallurgical Wastes (R. L. Folger, E. B. Sheldon, S. V. Castner, and E. R. Johns)

In the metallurgical processing of plutonium, wastes are formed which contain significant amounts of plutonium. Although this plutonium may be mixed with relatively large amounts of non-active contaminants, it has a high degree of radiochemical purity. Accumulation of these wastes provides a relatively large inventory of plutonium in a non-useful form. From each reduction of plutonium to produce a metal button, wastes in the form of reduction crucible fragments, packing sand, and the slag are obtained. These materials, containing two to three grams of plutonium per reduction batch, provide a large portion of the total bulk of the metallurgical wastes.

The plutonium recovery area at Savannah River is being designed by du Pont on the basis of a tentative flowsheet developed at ORNL[6], and on information available from Los Alamos, Hanford, and KAPL. Process development at ORNL has progressed to the pilot scale[7,8,9,10,11].

The crucible material and sand consist chiefly of magnesium oxide with two to four percent silica. The slag consists of calcium fluoride, calcium iodide, and metallic calcium. The ORNL process for recovery of plutonium from slag and crucible material involves dissolution of the material in nitric acid containing a measured amount of aluminum nitrate to control the amount of free fluoride obtained from the calcium fluoride present in the slag[8]. This fluoride is later complexed with excess aluminum nitrate and the plutonium removed from the bulk of the salts by solvent extraction[11]. The plutonium product from solvent extraction is concentrated by ion exchange methods and finally obtained in a form suitable for peroxide precipitation and return to metallurgical processing.

7.1 Slag and Crucible Dissolution

The work reported has consisted of a study in pilot scale equipment (Figure 7.11) of the dissolution procedure and preparation of a feed suitable for solvent extraction. In the development of the dissolution procedure, emphasis has been placed upon minimizing the loss of plutonium to the insoluble residue which consists of SiO_2 and corrosion products. The volatilization of various components of the dissolver solution has been observed. The filtration of the dissolver solution to remove the insoluble residue and provide a clear feed for solvent extraction has also received study.

In order to obtain the maximum recovery of plutonium from the slag and crucible wastes, it was desired to completely dissolve these materials including the plutonium. Nitric acid dissolves the magnesium oxide of the crucible and sand and also the components of the slag. The fluoride present in the slag dissolves the silica and aids in the dissolution of plutonium. The excess fluoride (approximately 0.1 to 0.2 M is complexed as hexafluoaluminate to permit solvent extraction of plutonium and reduce equipment corrosion.

In the dissolution procedure, nitric acid and a measured amount of aluminum nitrate are added to the dry charge pre-packaged in thin steel cans to reduce the hazard from radioactive dust while charging the dissolver. The solution is heated to about 120°C. During this period, some of the volatile components are removed by sparging (see Sections 7.11, 7.12, and 7.13). After the dissolution period, excess aluminum nitrate is added and the solution refluxed. The dissolver solution is filtered (see Section 7.14) and all of the residues are transferred from the dissolver to the filter. The combined residues are exhaustively leached with 65% nitric acid (or until the plutonium concentration in the leachings drops to 10^5 counts/min/ml), and this acid is recycled for subsequent dissolving. The residues were assayed for plutonium according to the method described in Appendix C.

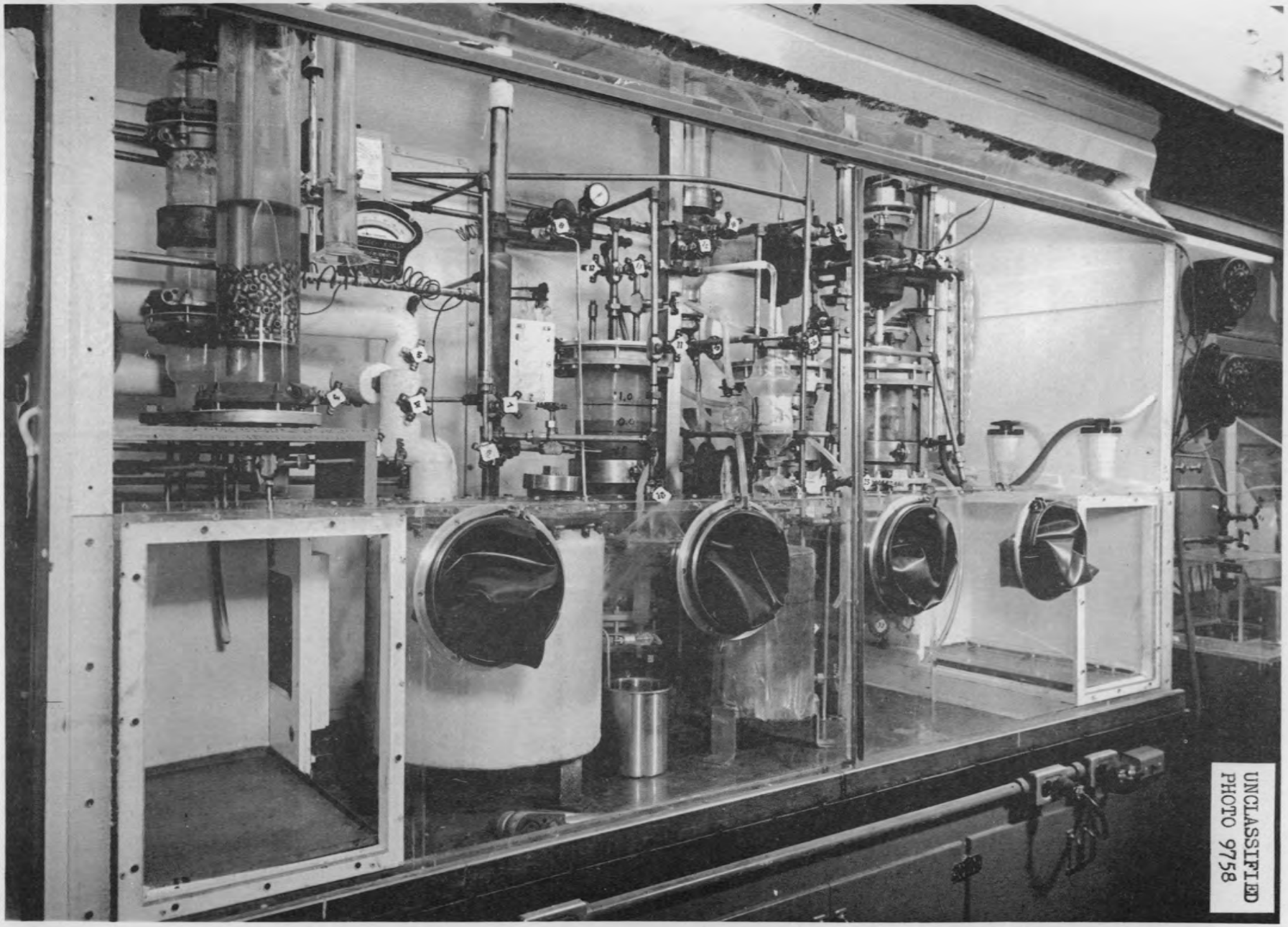

Figure 7.11
Slag and Crucible Dissolution Equipment

To date, six "hot" dissolution runs have been made in pilot scale equipment; one Los Alamos reduction crucible with associated sand and slag (total charge weight between 1.0 and 1.3 kilograms) was processed per run. Data pertaining to these runs are shown in Table 7.11.

The plutonium loss to the residue varied from 0.72% to 14.7%. It is noted (Table 7.11 and Figures 7.12, 7.13, and 7.14) that the high plutonium losses correspond to low dissolving times in the presence of free fluoride. When the fluoride is initially complexed by excess aluminum nitrate (Los Alamos procedure) the plutonium is not completely dissolved and losses to the residue are high[12]. A dissolution time of 90 minutes at 115° to 120°C gives 99% plutonium recovery.

7.11 Iodine Removal

In the course of the dissolution reaction, several components of the system are subject to volatilization. Removal of these materials may lessen the amounts of certain undesirable substances in the solution or reduce the bulk of the insoluble residue formed in the process. The presence of these volatile components in the off-gas stream requires provision for their suitable entrapment and removal. A caustic scrubber packed with stainless steel Raschig rings has been used to remove iodine, nitric acid, and volatile fluorides from the off-gas stream.

Iodine from the reaction of nitric acid with the calcium iodide of the slag may be volatilized; or, upon prolonged contact with the nitric acid at elevated temperature may be oxidized to iodate. The presence of large quantities of iodate in the dissolver solution is undesirable because of the low solubility of plutonium (IV) iodate and attendant loss to the insoluble residue. Iodate present in the feed for solvent extraction later may be reduced to iodine, causing corrosion problems.

Iodate may be removed by reduction with sodium nitrite followed by sparging of the resultant iodine. The initial formation of iodate may be minimized by starting the dissolution with dilute (6 to 8 molar) nitric acid and continuously sparging during the heating cycle. Sparge rates ranged from 0.1 to 1.0 cubic feet of air per minute at 4 psig. The liquid surface was approximately 13 inches in diameter and the off-gas line was one inch in diameter. Quantitative data on the residual iodine concentration after the initial sparge and again after the sodium nitrite reduction are being obtained.

7.12 Silica Removal

During dissolution the silica present in the crucible material and sand reacts with the fluoride from the slag to form fluosilicic acid. This compound is readily volatilized by steam distillation at 135°C[13]. Although the temperature of the dissolver solution only reaches 125°C, a significant amount of fluosilicic acid may be swept out during the sparging operation. This effect helps to reduce the fluoride concentration in the solution. Elimination of fluoride is essential because of its adverse effect on the extractability of

Figure 7.12

Temperature Variation and Fluoride Reaction Time
During the Dissolution Cycle: Run DG 2

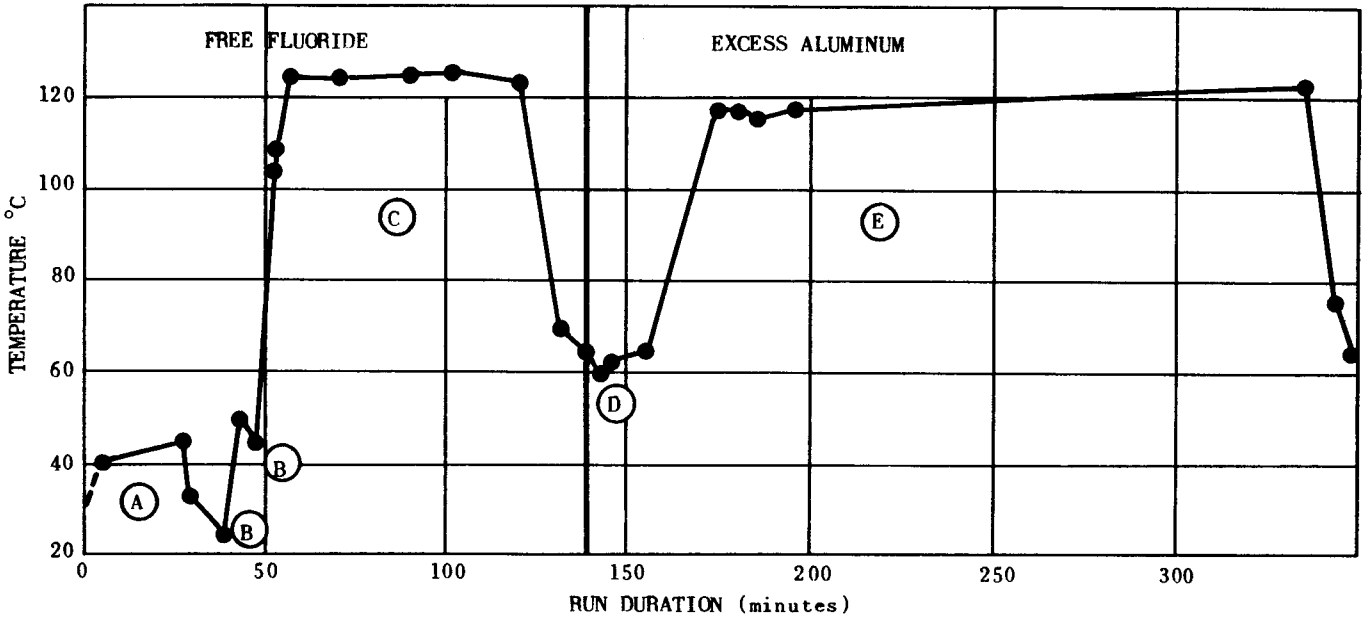

A Initial temperature rise due to exothermic reaction.

B Cooling and reagent addition (balance of HNO_3).

C Effective dissolution period, represented by area under curve above 80°C. (Includes iodine and fluosilicic acid distillation time).

D Cooling and reagent addition (ANN and $NaNO_2$).

E Second iodine distillation and SiO_2 digestion reflux.

Figure 7.13

Temperature Variation and Fluoride Reaction Time
During the Dissolution Cycle: Run DG 3

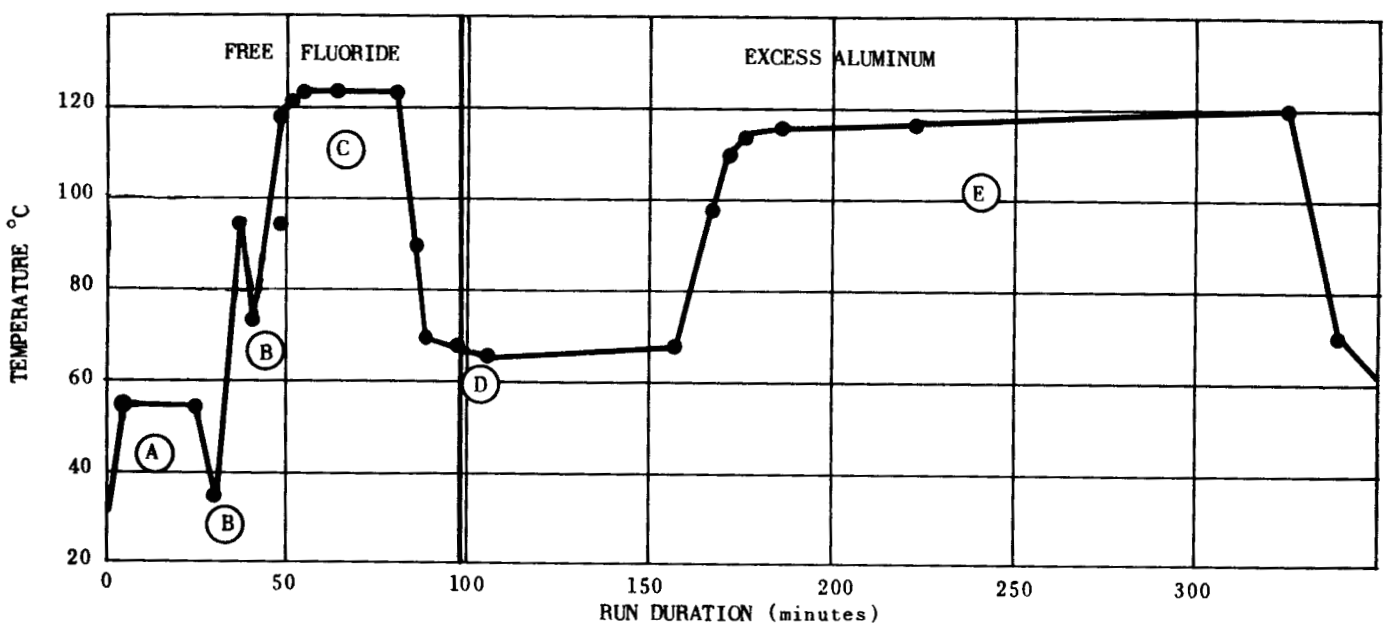

A Initial temperature rise from exothermic reaction.

B Addition of HNO_3.

C Effective dissolution period, represented by area under curve above 80°C. (Includes iodine and fluosilicic acid distillation time).

D Cooling and reagent addition.

E Second iodine distillation and SiO_2 digestion reflux.

Figure 7.14

Temperature Variation and Fluoride Reaction Time
During the Dissolution Cycle: Run DG 4

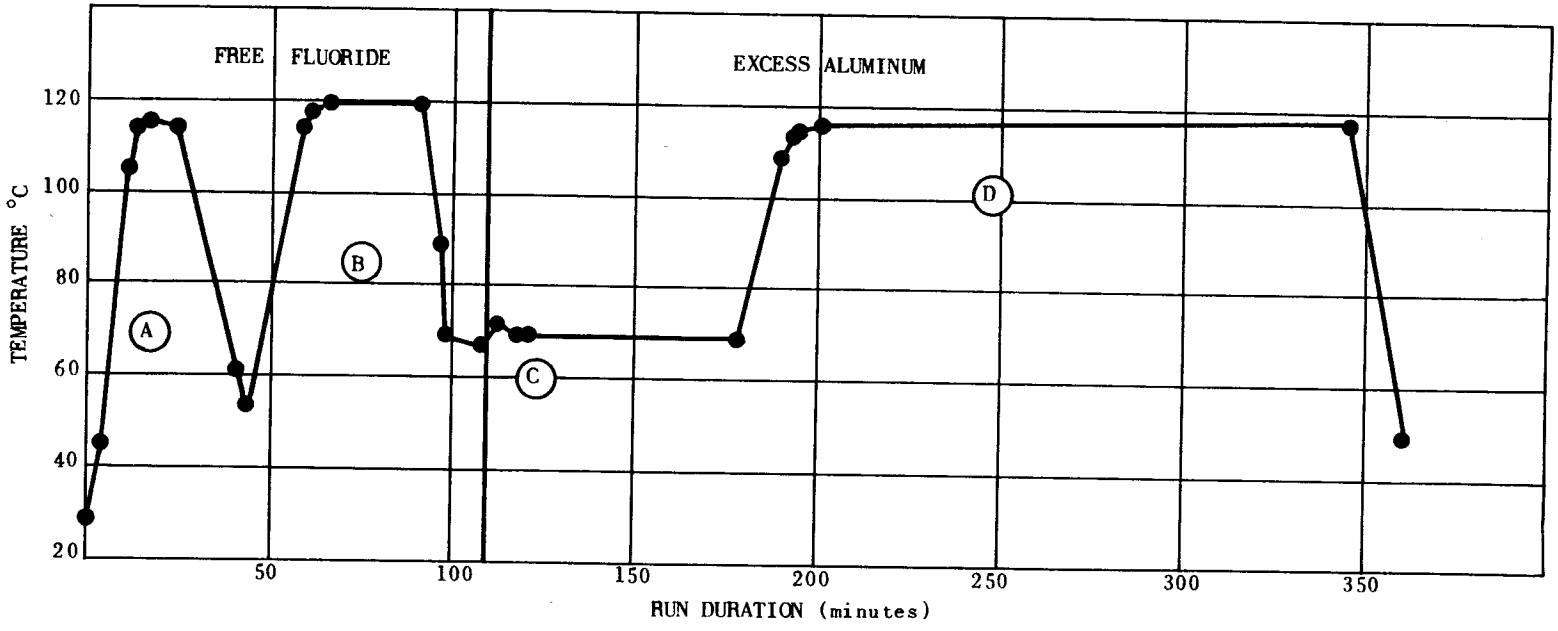

A Initial Reaction. Distillation of iodine from dilute HNO_3. Partial Dissolution.

B Completion of dissolution. Further distillation of iodine and fluosilicic acid. Full acid charge.

C Cooling. Addition of ANN and $NaNO_2$. Mixing.

D Final iodine distillation and SiO_2 digestion reflux.

Table 7.11

Slag and Crucible Dissolution Procedure Variables

Run No. DG:	1	2	3	4	5	6
Charge Wgt. (Kg)	1.062	1.081	1.248	1.029	1.230	1.049
Input HNO_3 (Conc'n.)[a]	67%	66%	64%	60%	62%	62%
Input HNO_3 (Kg/Kg Chg.)[b]	10.9	10.9	8.9	9.8	10.4	10.6
Dissolving Time (Min)	73	81	50	72	83	103
Total Pu Recovered (gm)	1.35	1.96	2.01	3.30	2.20	2.19
Pu Loss to Residue (%)	2.8	0.72	14.7	1.47	c	0.87

(a) Final concentration in weight percent HNO_3. The other constituent was H_2O.

(b) As 100% HNO_3.

(c) The residue from DG-5 was carried over to DG-6 as a heel. The percent loss to residue was measured on the basis of the total amount of plutonium recovered in both DG-5 and DG-6.

plutonium[11]. It was hoped that removal of silica by volatilization would allow recycle of the dissolution residues without a rapid build-up of insoluble material. The results of one such recycle experiment (see Table 7.12) show no decrease in the total residues. It is felt that the benefits to be gained by increased removal of silica do not justify the increased efforts required (longer volatilization time at higher temperature).

Table 7.12

Dissolution Residues

Run No. DG:	1	2	3	5	6
Charge Wgt. (g)	1,062	1,081	1,248	1,230	1,049
Residue Dry Wgt. (g)	16.5	20	18.5	b	42.7
Percent Heel[(a)]	68	81	65	b	82

(a) Based on the amount of SiO_2 which would be expected from the given charge.

(b) The residue from Run DG-5 was recycled to Run DG-6.

7.13 Loss of Nitric Acid

During the sparging operation some of the dissolver acid is distilled over to the caustic scrubber. In an attempt to estimate the amount of nitric acid lost to the off gas stream, the following reactions were postulated to occur in the dissolver:

(1) $MgO + 2\ HNO_3 \longrightarrow Mg(NO_3)_2 + H_2O$

(2) $Ca + 4\ HNO_3 \longrightarrow Ca(NO_3)_2 + 2\ NO_2 + 2\ H_2O$

(3) $CaI_2 + 4\ HNO_3 \longrightarrow Ca(NO_3)_2 + 2\ NO_2 + I_2 + 2\ H_2O$

(4) $CaF_2 + 2\ HNO_3 \longrightarrow Ca(NO_3)_2 + 2\ HF$

(5) $Al + 6\ HNO_3 \longrightarrow Al(NO_3)_3 + 3\ NO_2 + 3\ H_2O$

(6) $Fe + 6\ HNO_3 \longrightarrow Fe(NO_3)_3 + 3\ NO_2 + 3\ H_2O$

This list of reactions is not intended to be a complete description of the processes occurring in the dissolver. It is useful, however, for calculation of the amount of nitric acid consumed. It was assumed that the slag and crucible weight was constant from run to run and that the variation in charge

weight was due to variation in the amount of packing sand used in the reduction bomb. Data from which the calculations were made are presented in Tables 7.13 and 7.14 below. The nitric acid loss by volatilization varies, averaging about ten percent.

Table 7.13

Theoretical Nitric Acid Requirements for Dissolution

Constituent	Wgt (g)[a]	Moles	Factor[b]	Moles HNO_3 Required
Slag	366			11.09
Ca	42	1.05	4	4.20
CaF_2	207	2.65	2	5.30
CaI_2	117	0.398	4	1.59
Crucible-MgO	460	11.4	2	22.8
Reduction Bomb Gasket-Al	5	0.185	6	1.11
Charging Can-Fe	20	0.358	6	2.15
Total				37.15

(a) Based on slag composition reported in Reference 12.

(b) Based on equations presented in Section 7.13.

Table 7.14

Nitric Acid Material Balance for Dissolution

Run No. DG:	3	4	5	6
Charge Wgt (g)	1,248	1,029	1,230	1,049
Estimated Wgt Sand (g)[a]	409	190	391	210
HNO_3 required for sand (m)[b]	19.4	9.0	18.6	10.0
Total HNO_3 required (m)[c]	56.6	46.2	55.8	47
Total HNO_3 added (m)[d]	176	160	204	176
HNO_3 in solvent extraction feed (m)[e]	93.5	99.0	113	129
HNO_3 volatilized (m)[f]	26	15	35	0
HNO_3 volatilized (%)	15	9.4	17	0

(a) The combined slag and crucible weight including SiO_2 and other minor constituents is taken to be 839 grams.

(b) Assuming the sand to be 96% MgO requiring 2 moles HNO_3 per mole of MgO for dissolution.

(c) Includes 37.15 moles shown in Table 7.13.

(d) Taken from Table 7.11.

(e) Taken from Table 7.15.

(f) Obtained by difference.

7.14 Feed Adjustment

The dissolver solution as such would not be suitable for solvent extraction, since (1) the solution is super-saturated with salts and solidifies at room temperature, (2) the free fluoride concentration severely represses the plutonium (IV) distribution coefficient when extracted by TBP, and (3) the high acidity might cause excessive deterioration of the solvent. Conditions (1) and (3) are eliminated by dilution of the solution with water. Condition (2) is remedied by the addition of excess aluminum nitrate to complex the fluoride. The addition of 1.2 moles of aluminum nitrate per mole of fluoride initially present in the slag has been found to give plutonium distribution coefficients (O/A) of about 50. However, this method of complexing the fluoride introduces a new problem because the silica formerly held in the solution as fluosilicate ion now settles out as finely divided, hydrated SiO_2. This siliceous material may cause severe emulsion problems in the contactors used for solvent extraction.

In the six dissolution runs performed to date, sodium nitrite solution has been added to reduce iodate (section 7.11). This provides some of the dilution water needed to reduce the acidity and also to prevent solidification of the solution. The total amount of dilution water, including that obtained from the addition of 1.6 M $Al(NO_3)_3$, and the resultant acidities are listed in Table 7.15. The amount of aluminum nitrate added in Run DG-1 was apparently insufficient to give a satisfactory plutonium distribution coefficient into the organic phase. In the other runs satisfactory feeds were obtained by dilution and aluminum nitrate addition.

7.15 Feed Clarification

Filtration has been studied as a means of removing the siliceous material from the feed. Coarse fritted Pyrex with a Fiberglas 183 glass cloth prefilter, porosity "E" sintered stainless steel, and porosity "E" sintered stainless steel with a glass cloth prefilter were used as filter media. No filter aid was used. Plugging occurred in four of the six runs, which increased the filtration time to 24 hours. In the other two runs, filtration times of one hour or less were obtained using a 4 inch diameter filter. The best results were obtained with the sintered stainless steel filter backed with the glass cloth prefilter. It was found that the time allowed for digestion and dehydration of the reprecipitated silica (by refluxing at 120°C) materially affected the filtration. Residues from runs involving 2.5 hours digestion time were slimy in appearance and showed a tendency to plug the filter. In the run for which 9 hours digestion time was used, the residue was granular and filtration was rapid. Complete clarification of the solutions has not yet been obtained; some solids have settled out of the filtrates upon standing. All of the filtrates, however, were processed through batch countercurrent equipment satisfactorily.

Further study of the filtration step is planned. Various filter media with and without filter aids and precoats will be tested in an effort to develop a more satisfactory procedure.

Table 7.15

Solvent Extraction Feed Preparation

Run No. DG:	1	2	3	4	5	6
Diluent H_2O (Kg)	9.67	10.14	9.54	6.54	7.79	9.64
$Al(NO_3)_3$ (Kg)	0.955	1.36	1.36	1.36	1.36	1.36
Final volume (l)	20	20.5	18.7	17.1	19.0	21.6
Feed Acidity (M)	6.7	6.0	5.0	5.8	5.95	5.94
D. C. (Pu E_A^0)[a]	30	53	40	82	52	(130)[a]

(a) Analytical results doubtful. Value appears high.

7.2 Solvent Extraction

The primary object of the work was the isolation of several grams of plutonium from slag and crucible solution under the proposed flowsheet conditions[6]. It was desired to test the flowsheet in continuous solvent extraction equipment, but neither continuous equipment nor the space to set it up was available. Therefore, it was necessary to process the slag and crucible solution in batch countercurrent equipment (see Figure 7.21). Nine 1 liter contactors, equipped with interface stirrers, were connected so that all solution transfers could be made by vacuum. Solution was processed under conditions analogous to the Purex Second Plutonium Cycle[14]; these conditions are shown in Figures 7.22 and 7.23.

7.21 Feed Preparation

The slag and crucible dissolution procedure is designed to give a feed solution that is ready for solvent extraction. A sample of each batch of feed was equilibrated with 30% TBP in Amsco, and the plutonium distribution coefficient was determined before the countercurrent extraction was begun. No adjustment of the feed was required for pilot scale solutions DG-2 through DG-6 (see Section 7.14). The composition of the feed solutions is listed in Table 7.21. These compositions correspond closely to that specified in the tentative

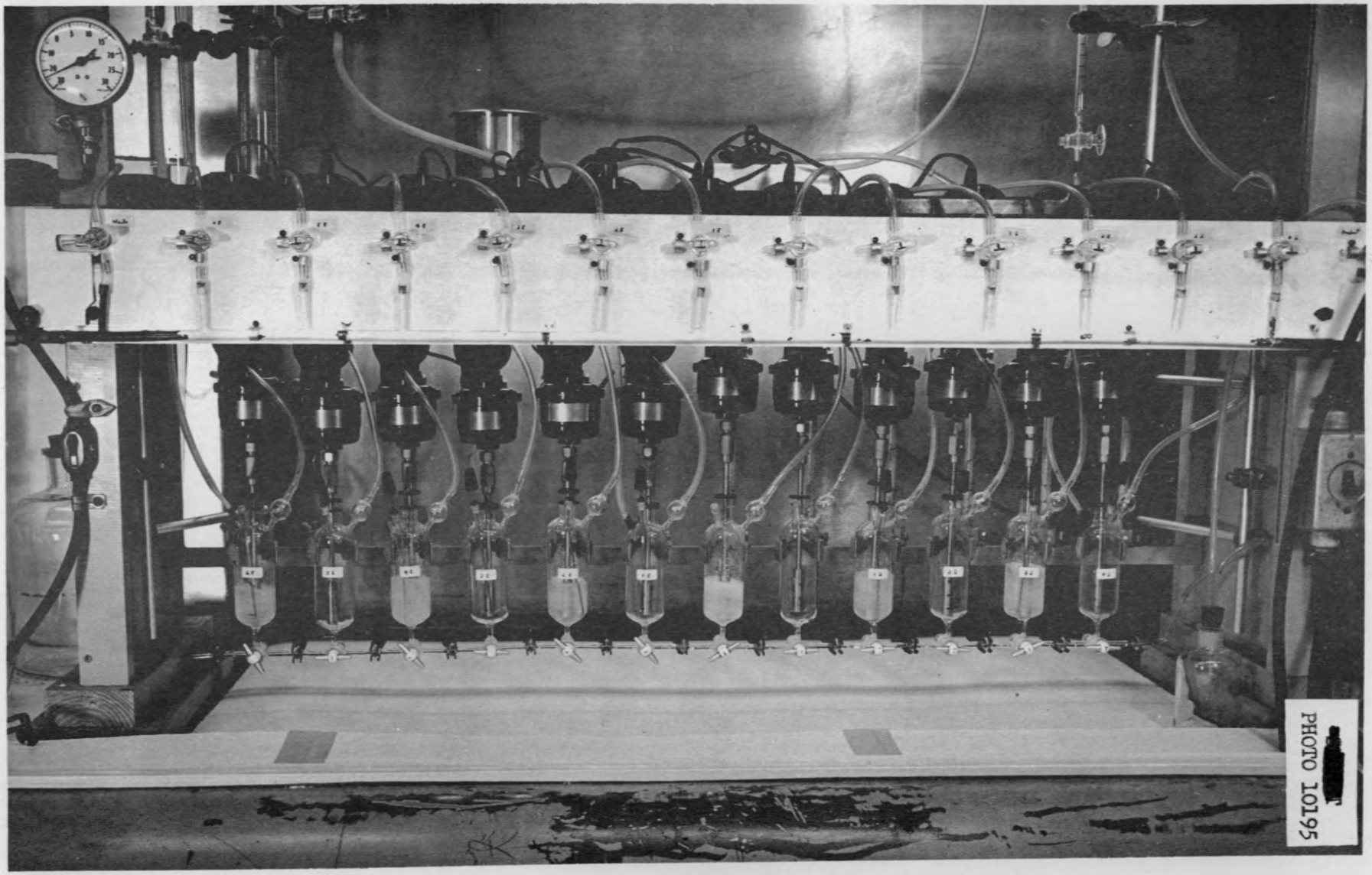

Figure 7.21
Batch Countercurrent Apparatus for Solvent Extraction

Figure 7.22

EXTRACTION CONDITIONS – SLAG AND CRUCIBLE SOLUTION

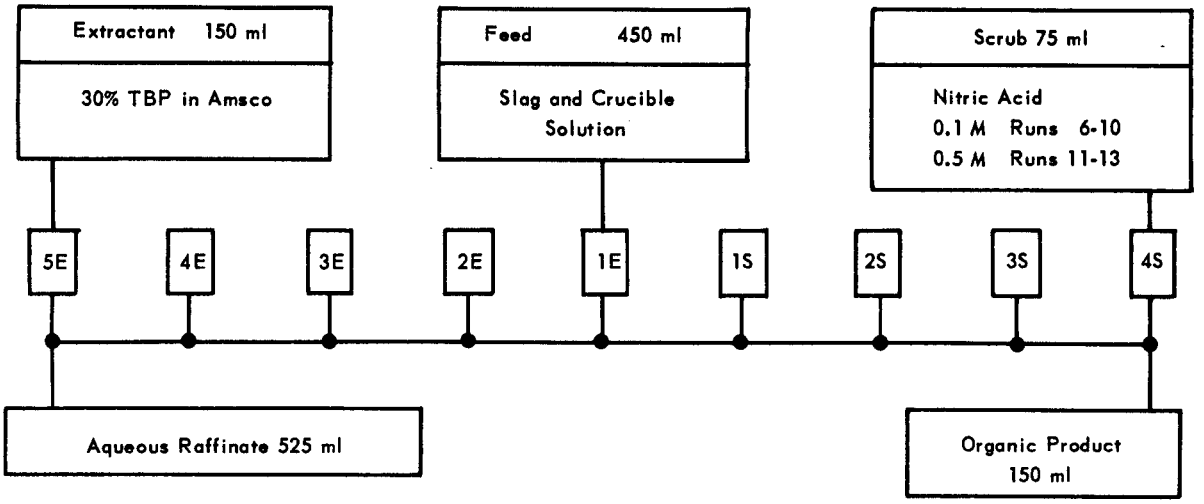

75 equilibrations (average)
2 to 3 minute contact time

Figure 7.23

STRIPPING CONDITIONS – SLAG AND CRUCIBLE SOLUTION

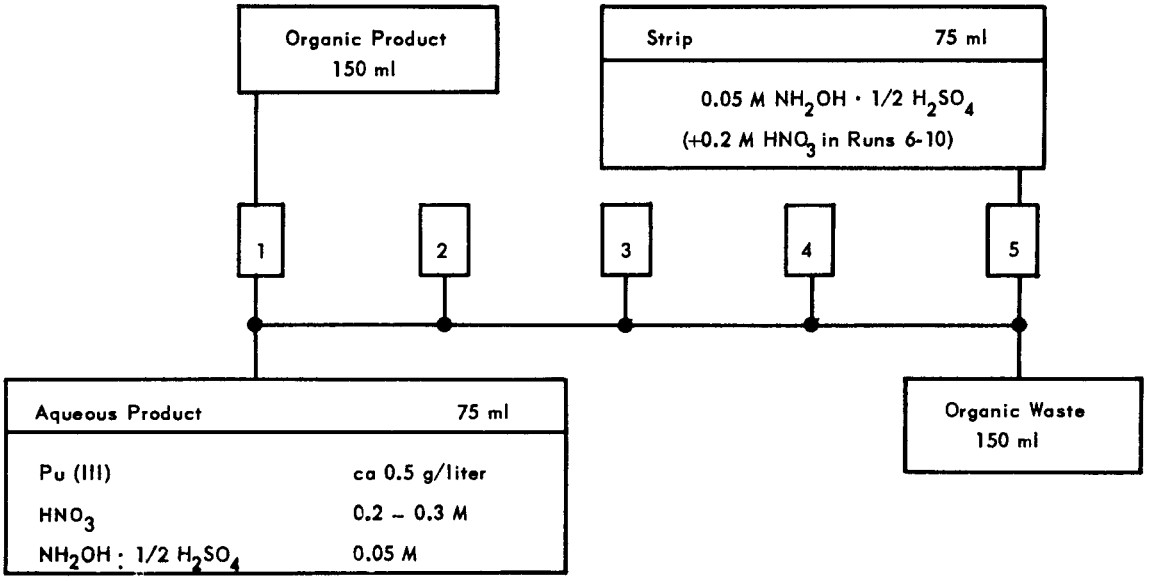

25 equilibrations (minimum)
2 to 3 minute contact time

● Valves

flowsheet[6], with the exception of Mg^{++} concentration. SRP residues will give a solution containing about 1.2 M Mg^{++}; Los Alamos residues, which contain a smaller amount of MgO "sand", give between 0.8 and 1.1 M Mg^{++}.

Table 7.21

Composition of Feed Solutions for Batch Countercurrent Extraction

BCE No.	S & C Solution Number	Al[(1)] M	Ca[(2)] M	Mg[(2)] M	HNO_3[(3)] M	Pu[(3)] (g/l)
6	DE-3, 6, 7, 8	0.26	0.19	1.0	6.2	0.187
7	DG-1	0.32	0.19	0.79	5.95	0.059
8	DG-2	0.33	0.21	0.86	5.5	0.081
9	DG-3	0.36	0.22	1.14	5.0	0.078
10	DG-4	0.39	0.24	0.94	5.7	0.170
11	DG-5	0.35	0.22	1.10	5.8	0.113
12	DG-6	0.33	0.21	0.82	6.4	0.100
13	(Clean-up)	--	--	--	6.0	0.010

(1) Calculated from amount of ANN used in dissolution. cf Appendix D.

(2) Calculated from weight and reported composition of slag and crucible residues. cf Appendix D.

(3) By analysis

HNO_3 - titration

Pu - gross alpha counting

7.22 Extraction and Stripping

The data obtained in the batch countercurrent extraction runs are summarized in Table 7.22. Feed for run 6 was a composite of solutions prepared by small-scale dissolutions in a 2-liter Pyrex dissolver. In the other runs, the solution from each pilot scale dissolution (ca 20 liters) was processed individually. Determination of the plutonium IV distribution coefficient (O/A) for the feed solutions normally gave values of about 50. Solutions DG-4 and DG-6 showed unusually high values for the D.C., but these were probably caused by inaccurate analysis of the aqueous phase. The extraction loss in run 7 was abnormally high (0.16%); this was attributed to inefficient stirring of the solutions, and the condition was corrected. In addition, the contacting time was increased from two minutes to three. The low stripping loss of 0.0004% in run 6 is in agreement with that found in previous countercurrent runs[11]. Runs 7 through 12 showed increasingly large loss of plutonium to the organic waste. These losses are believed to be caused by excessively long storage (from 2 to 30 days) of the organic product, necessitated by the fact that the same contactors were used for extraction and for stripping. Normal operation in continuous solvent extraction equipment would eliminate this situation so that low stripping losses are to be expected in plant operation.

7.23 Settling Time

Phase separation in the extraction of slag and crucible solution is generally slower than it is for Purex feeds; coarse emulsions occasionally are found in the organic phase, and settling time as long as 120 seconds may be required for complete phase separation. Silica is believed to be responsible for the long settling times, but it is difficult to fix a limit for the amount of silica that can be tolerated in the filtrate from the slag and crucible dissolution. This difficulty is caused by the fact that colloidal silica is probably responsible for emulsification[11], whereas analysis of the solution indicates only the amount of dissolved silica present. Work done at Hanford[15] showed little or no correlation between settling and the concentration of silica found by analysis.

Settling times have been measured in the batch countercurrent equipment; typical values are listed in Table 7.23. The maximum settling time encountered was 110 seconds in the first extraction stage (feed plate) of BCE Run 12. Because settling times are of great importance in the design of mixer settlers for the SRP recovery area, KAPL has evaluated "cold" slag and crucible solution in the Midi unit, and "hot" solution in Mini. On the basis of the mixer settler runs, which showed a maximum settling time of 120 seconds with fresh solvent and 150 seconds with recovered solvent, 180 seconds was taken by KAPL as the basis for design of the settling section[16].

[redacted]

Table 7.22

Summary of Batch Countercurrent Extraction Results

BCE Run No.	Pu E^{O}_{A}	Extraction Loss (Composite)	Stripping Loss (Composite)	Approx. Pu Wt. in Product solution (grams)	Ionic Impurities in Product Solution Cation/Pu by Wt.				Ionic Decontamination Feed to Product		
					Al	Ca	Fe	Mg	Al	Ca	Mg
6	50	0.02	0.0004%	1.17	.0029	.075	.0031	.0195	12,000	508	6,300
7	52	0.16	0.02	0.76	.0175	.183	.0175	.092	5,800	740	3,700
8	45	0.03	0.02	1.24	.0060	.106	.0077	.0408	10,300	730	4,800
9	32	0.02	0.05	1.12			ANALYSES NOT YET COMPLETE				
10	82	0.04	0.48	2.14							
11	52	0.04	0.78	2.87							
12	100	0.05	1.38	2.37							
13			1.3	0.49							

[redacted]

Table 7.23

Time Required for Complete Phase Separation in Batch Countercurrent Extraction of Slag and Crucible Solution

Run	5E	4E	3E	2E	1E	1S	2S	3S	4S
BCE 7 (DG 1)	65	60	55	55	55	60	55	70	55
BCE 8 (DG 2)	60	65	55	55	45	45	45	40	30
BCE 10 (DG 4)	80	70	70	90	100	35	45	45	50
BCE 12	100	90	90	95	110	45	45	45	50

7.24 Product Purity

The product solutions were analyzed spectroscopically, after removal of plutonium by extraction with TTA. Complete results of the analyses, listed in Table 7.24 show that calcium is the principal contaminant. The product purity is comparable to that obtained in the ORNL Pilot Plant Purex run HP 13, although it is much poorer than that obtained in more recent Purex runs HCP 1, 2, and 4, (Table 7.25). Pending evaluation of the plutonium product at Los Alamos, it is assumed that the purity is adequate.

Table 7.24

Analysis of Product Solutions

Cation	Batch Countercurrent Extraction Run		
	6	7	8
Pu	1090 ppm	273 ppm	414 ppm
Al	3.2	4.8	2.5
B	trace	trace	trace
Ca	82	50	44
Cr	3	3	5
Cu	trace	trace	trace
Fe	3.4	4.8	3.2
Mg	21.3	25.2	16.9
Na	<100	<100	<100
Ni	< 1	< 1	< 1
P	trace	trace	trace
Pb	<20	< 20	< 10

Table 7.25

Comparison of Plutonium Product Purity with Purex IIBP

Percent by weight based on Pu

	BCE Runs			Purex Runs				
	6	7	8	HP-13	HCP-1	HCP-2	HCP-3	HCP-4
Al	0.29	1.75	0.60	0.4	0.07	0.07	0.12	0.32
Ca	7.5	18.3	10.6	30	1.23	1.17	23.1	1.93
Mg	19.5	9.2	4.1	8	0.01	0.08	0.86	0.25

7.3 Product Concentration by Ion Exchange

The plutonium product from BCE runs 5-13 has been absorbed on a 60 ml bed of Dowex-50W resin in batches of about 4 grams each. The product in the first two batches was eluted with 6 M nitric acid, 0.3 M sulfamic acid; the bed was reconditioned after elution and then used for absorption of the next batch. Elution of the third batch is now in progress.

7.4 Corrosion Studies

The choice of a satisfactory material for fabrication of the metallurgical waste dissolution equipment is particularly important since the material must withstand a corroding medium containing nitric acid, hydrofluoric acid, and iodine in concentrations which vary widely as the dissolution proceeds. Initially, a series of survey corrosion tests were conducted with a group of materials considered desirable for this application. As a result of this work, stainless steel type 309 Cb was chosen for further testing to determine its life expectancy under the conditions met in the dissolver and auxiliary equipment.

7.41 Survey Tests

Several types of stainless steel and one type of glass (Table 7.41) were prepared for exposure according to the following procedure. The samples (dimensions: 2 x 1 x 1/4 inch; approximate weight: 50 grams) were cleaned by (a) boiling in carbon tetrachloride followed by a water rinse, (b) boiling in concentrated nitric acid followed by a second water rinse, and (c) a second boiling in carbon tetrachloride. After drying and cooling, the samples were weighed to

± 0.1 mg and measured to ± 0.001 inch, from which the volume, surface area, and density were calculated. The samples were suspended on platinum wires encased in fluorothene tubing (for electrical insulation), which were suspended from hooks in the top of a type 347 stainless steel dissolver. Wherever possible, one coupon was suspended in the vapor zone, one at the interface, and one completely submerged.

The corrodent mixture was that obtained by following the metallurgical waste recovery flowsheet[6] at 1/100 scale until the final iodine sparging was completed. The solution was then refluxed for the remainder of a 24-hour period (approximately 16-18 hours). From the weight loss, density, and area, the penetration in inches/year was calculated assuming 365 - 24 hour periods of the same corrosion as described.

In Table 7.41 are listed the results obtained by the survey tests. The penetration is the average penetration from two such corrosion cycles as described above.

It is seen that, under the conditions imposed by the metallurgical wastes dissolution procedure, the corrosion resistance of type 309 Cb stainless steel is generally superior to that of other materials tested. The resistance of stainless steels type 329 and its alloys is comparable to that of 309 Cb; the former, however, were eliminated because of fabrication difficulties and nonavailability.

7.42 Durability Tests

For the durability testing of type 309 Cb the samples were prepared in the following manner. Six of the nine samples (#4-9) were cut in half, welded together, heated to 2100°F for thirty minutes and quenched in water. The surfaces of the samples were ground smooth. The samples were cleaned as described previously, weighed, and measured. Three of the welded samples (Nos. 7, 8, and 9) were pickled at the same time as the testing dissolver, which was constructed of type 309 Cb and heat treated. A crack was now readily apparent in the weld of sample #7 although before pickling, none of the welds could be observed visually. The nine samples were photo-micrographed after cleaning and weighing. The three samples which had been pickled were rephotomicrographed after pickling. The welded samples were also X-rayed.

It is planned to expose all the samples for ten 24 hour corrosion cycles; the results of five cycles of exposure are shown in Table 7.42. It is seen that the performance of welded and welded-pickled specimens is equal to that of the unwelded samples. The average penetration rates of the unwelded samples (0.028, 0.022, and 0.015 inches per year in the vapor, liquid, and at the interface) are somewhat lower than the corrosion measured for 309 Cb in the survey tests.

Table 7.41

Survey Corrosion Tests of Various Materials

Sample Type	Penetration (inches/year)			Remarks
	Vapor	Liquid	Interface	
Pfaudler glass	.065	.080	?chipped	
SS #304 ELC	.046	.030	.030	No pitting observed.
SS #309 Cb	.028	.030	.025	No pitting.
SS #309 Cb		.023		No pitting welded sample.
SS #316 ELC	.120	.062		Badly pitted.
SS #347	.047	.035	.040	
SS #329	.030	.018	.028	Sample in liquid was of low density.
SS #329 V	.027	.018		SS 329 alloyed with vanadium.
SS #329 Ti	.032	.020		SS 329 alloyed with titanium.
SS #329 Al			.019	SS 329 alloyed with aluminum.
Carpenter #20	.045	.028		

Table 7.42

Duration Tests of SS Type 309 Cb

Sample No.	Penetration (inches/year)			Remarks
	Vapor	Liquid	Interface	
1, 2, 3	.028	.022	.015	Unwelded samples. No pitting
4, 5, 6	.031	.024	.016	Welded samples. Some pitting on No. 4.
7, 8, 9	.027	.018	.014	Welded-pickled samples. No pitting. Sample No. 7 had a crack in the weld presumed due to poor welding.

8.0 Denitration of the Uranium Product (V. J. Reilly)

During September of 1951, 4530 pounds of uranyl nitrate collected from initial Purex Pilot Plant demonstration runs was processed to the orange oxide (UO_3) at the Mallinckrodt Chemical Works in St. Louis. Du Pont personnel, who observed the operation, reported that when the first charge was calcined, excessive foaming occurred within five minutes of startup causing loss of about 50% of the charge.

Subsequent laboratory investigation disclosed that traces of dibutyl acid phosphate (DBP), formed by hydrolysis of entrained solvent present in the Purex uranium product during evaporation, was responsible for the foaming. Consequently it was recommended that after-separators be installed on the uranium strip contactors to minimize the carry over of solvent with the aqueous uranium stream.

8.1 Foaming Studies

Samples of second cycle uranium product (EU boildown) from recent Pilot Plant runs made following the installation of after-separators on the uranium strip columns, were evaporated beyond the initiation of denitration with no tendency to foam. Two samples of drummed product were also denitrated to this same extent, one of which exhibited slight foaming. These results show promise that, with the present care in eliminating entrainment of solvent from the IEU stream, no trouble will be encountered due to foaming during denitration.

8.2 Ruthenium Behavior

Conditions during denitration (high temperature with an atmosphere of nitric acid, nitric oxide and oxygen) appear to be more favorable for ruthenium oxidation to RuO_4 than are present in boiling concentrated nitric acid, which has been demonstrated in connection with acid recovery to be favorable for this oxidation. In the denitration test at Mallinckrodt in September, 1951, about 90% of the ruthenium was lost in the conversion of uranyl nitrate to UO_3. To determine roughly the extent of this distillation, as well as the ultimate resting place for this ruthenium, denitration of EU and CU concentrate were carried out in the equipment set up to investigate foaming. The agitation was powerful enough to carry the reaction to about 90% of completion (gauged by the quantity of nitric acid and NO_2 absorbed in the scrubber), but not powerful enough to carry the product to a powder which could be removed from the flask. The uranium trioxide was recovered from the flask by dissolution in nitric acid, so that adherence of ruthenium to the surfaces in the flask was not investigated.

Three samples of uranyl nitrate solutions from the Purex pilot plant were denitrated in this equipment. Second cycle product from runs HCP 2 and HCP 2A gave ruthenium decontamination factors of 5 and 3.9, respectively. A sample of 1CU concentrate (HCP 3) on denitration yielded a ruthenium DF of 13. In all these runs the gross gamma and ruthenium balance was better than 95%, with the activity removed from the uranium found in the acid absorber. Essentially no ruthenium distilled before denitration began.

In order to determine if appreciable ruthenium would be held up on the surface of metal equipment, a 347 stainless steel delivery tube was fabricated to conduct the vapors from the flask to the receiver. It served as condenser in the latter half of its length by virtue of a water jacket. In addition to this metal vapor tube, the glass flask stirrer was replaced with one made from stainless steel. Two runs were made in this part-stainless equipment using aliquots of the uranyl nitrate solution obtained for the foaming studies. The ruthenium DF averaged 3.0, and the ruthenium beta and gross gamma balance (pot to scrubber) was essentially 100% indicating no hold-up in the vapor line.

These results are believed to indicate roughly the lower limit to expect for ruthenium decontamination during denitration. It should be a lower limit since more ruthenium would be expected to distil if the denitration were carried to completion. Likewise, if there is hold-up on stainless steel surfaces in the pot, this will contribute to the DF in a plant-size denitrator, as only the loose product is withdrawn (in contrast to the laboratory method of dissolving all the UO_3 to obtain a sample).

9.0 Chemical Stability of Solvent Diluent (L. E. Line, Jr.)

In the ORNL Pilot Plant it has been observed that the solvent becomes yellow with continued recycling, and this has been attributed to the nitration of some of the aromatic components. Some exploratory work, described below, was carried out to determine what might be responsible for the discoloration. The conditions were intended to simulate those in the IIA column.

(a) Forty ml of 6 M HNO_3 shaken with 10 ml of 30% TBP in Amsco 123-15 for 10 minutes gave no yellow discoloration in the organic phase.

(b) Forty ml of 0.1 M HNO_2 (freshly prepared) shaken with the solvent mixture under the same conditions showed no color.

(c) Twenty ml of 12 M HNO_3 + 20 ml of 0.2 M $NaNO_2$ shaken with 10 ml of the solvent mixture imparted a pale yellow color to the organic phase within five minutes. This color was largely unaffected by washing with water or saturated Na_2CO_3 solution.

(d) Ten ml of TBP shaken with 20 ml of 0.2 M $NaNO_2$ + 20 ml 12 M HNO_3 gave a pale yellow color to the organic phase that was readily washed out with water.

(e) Similar results were obtained with TBP and diluent using N_2O_4 gas. In the case of Amsco much of the discoloration was removed by washing, but a permanent pale yellow color remained.

These facts suggest that the observed discoloration is associated neither with the HNO_3 nor with HNO_2 alone but with the HNO_3 - HNO_2 system. Furthermore, the permanent discoloration appears to be associated with the diluent and not with the TBP.

Nitrogen oxides, which would be present as a result of the reaction between HNO_2 and HNO_3, are known[17] to nitrate aromatics and olefins and also to oxidize carbon side chains of aromatic nuclei to carboxylic acids at room temperature, although the reactions are slow and the yields are slight. Nevertheless, significant damage to the solvent is a possibility where the solvent is recycled many times. Apart from the oxides, the system HNO_3-HNO_2 is an oxidizing one and this may contribute to chemical degradation of the solvent. Some experiments are to be carried out to determine nitrogen fixation by the solvent over prolonged contact with nitric acid containing nitrous acid corresponding to the IIAF stream.

10.0 Nitrous Acid Behavior during Solvent Extraction (L. E. Line, Jr.)

10.1 Extraction of Nitrous Acid

Since HNO_2 appears to be essential to the discoloration of the solvent, it seemed important to determine whether the reactions occur only on contact between aqueous and organic phases or whether they take place in the organic phase. After preliminary results showed a large tendency for nitrous acid to be adsorbed, indicating that the reaction probably occurs in the organic phase, an attempt was made to obtain reliable values of the distribution coefficient under various conditions, since knowledge of the behavior of nitrous acid seemed fundamentally important in the Purex Process.

An experiment was carried out to determine whether sodium nitrite is extracted by Purex solvent from a neutral solution. Analysis of aqueous phases before and after extraction showed a loss of 5% of the nitrite and indicates that the nitrite is extracted as HNO_2 rather than as $NaNO_2$.

10.11 Instability of Nitrous Acid

Initial experiments to determine the distribution of HNO_2 between organic and aqueous phases under conditions specified for the ORNL Flowsheet #3 IIA column extraction (IIAF: 0.1 M HNO_2, 6 M HNO_3) were unsuccessful because of the rapid decomposition and oxidation of the nitrous acid. Analyses

showed 57% HNO_2 decomposition when 90 ml of 6 M HNO_3 - 0.1 M HNO_2 was shaken for 20 minutes (160 ml of air). Comparable results were obtained in a similar experiment omitting nitric acid. When air was excluded the rate of disappearance of HNO_2 was diminished somewhat but not altogether.

Nitrous acid probably decomposes according to the equation

$$3\ HNO_2 \rightleftharpoons 2\ NO + H_2O + H^+ + NO_3^-$$

In the presence of a high concentration of HNO_3, nitrous acid appears to be completely unstable,[18] but for low concentrations of HNO_3, the latter may be expected to stabilize the HNO_2 through the common-ion effect. Accordingly, it was decided to extract and measure the distribution coefficients under the following conditions (a) a minimum of 10 - 15 ml free space (filled with nitrogen) to reduce the formation of NO, (b) 0.01 M instead of 0.1 M HNO_2 and (c) 1 M instead of 6 M HNO_3. The method and calculations used to determine nitrous acid distribution are described in Appendix E. Such conditions served to reduce the decomposition to a few percent, as may be seen from Table 10.1.

Table 10.1

Decomposition of 0.01 M Nitrous Acid under Various Conditions

Expt.	Shaking Time (min)	HNO_3 (M)	Free Space (ml)	HNO_2 Decomposed (%)
1	30	1	180	17
2	25	1	45	3
3	10	0	45	13.5
4	10	6	45	10
5	60	3	15	2
6	75	1	15	0

10.12 Determination of Distribution Coefficient

Table 10.2 shows that the extraction of HNO_2 is due almost entirely to the tributyl phosphate, there being only a slight tendency for extraction by Amsco alone. The distribution coefficient of around 21 is rather high; it is approximately 100 times that of nitric acid.

However, the distribution coefficient varies markedly with the concentration of nitric acid, as may be seen from Table 10.3 and the accompanying plot (figure 10.1). It appears that as the molarity of the nitric acid is increased from 0 to 6, the distribution coefficient goes through a maximum of around 21 in the neighborhood of 1 M and drops to a value of 3 at 6 M. The reason for this behavior, especially the initial rise in distribution coefficient is not clear. The decrease may be related to the predominance of HNO_3 over HNO_2 in the competition for complex formation with TBP, or simply the predominance of HNO_3 over TBP in the competition for HNO_2 as a result of increasing ionic strength of the aqueous phase.

Table 10.2

Nitrous Acid Extraction by AMSCO, TBP, and 30% TBP in AMSCO

Aqueous: 90 ml of 0.01 M HNO_2 in 1 M HNO_3

Organic: 35 ml, as indicated

Solvent	Shaking Time (min)	D_1	D_2	DC (O/A)
AMSCO 123-15	5	0.352	0.312	0.33
	10	0.356	0.283	0.66
	15	0.335	0.270	0.62
	25	0.350	0.295	0.48
TBP	5	0.367	0.042	20.0
30% TBP in AMSCO	5	0.378	0.038	23.0
	10	0.367	0.043	19.4
	20	0.368	0.042	20.0

D_1 = optical density of aqueous phase before extraction.

D_2 = optical density of aqueous phase after extraction.

$$DC\ (O/A) = \frac{D_1 - D_2}{D_2} \quad \frac{Va}{Vo}$$

$\frac{Va}{V_o}$ = volume ratio aqueous:solvent.

[redacted]

Table 10.3

Nitrous Acid Extraction by 30% TBP in AMSCO

Aqueous: 90 ml of 0.01 M HNO_2 in HNO_3 of various concentrations

Organic: 35 ml of 30% TBP in AMSCO 123-15

HNO_3 M	Shaking Time (Min)	D_1	D_2	DC (O/A)
0	10	0.394	0.062	13.8
0	10	0.405	0.056	16.0
0.5	10	0.367	0.043	19.4
1	5	0.378	0.038	23.0
1	10	0.367	.043	19.4
1	20	0.368	.042	20.0
3	10	0.375	0.087	8.5
6	10	0.385	0.177	3.0

D_1 = optical density of aqueous phase before extraction.

D_2 = optical density of aqueous phase after extraction.

$$DC\ (O/A) = \frac{D_1 - D_2}{D_2} \times \frac{Va}{Vo}$$

$\frac{Va}{Vo}$ = volume ratio aqueous: solvent.

FIG. 10.1

NITROUS ACID DISTRIBUTION BETWEEN PUREX SOLVENT MIXTURE & NITRIC ACID OF VARIOUS CONCENTRATIONS

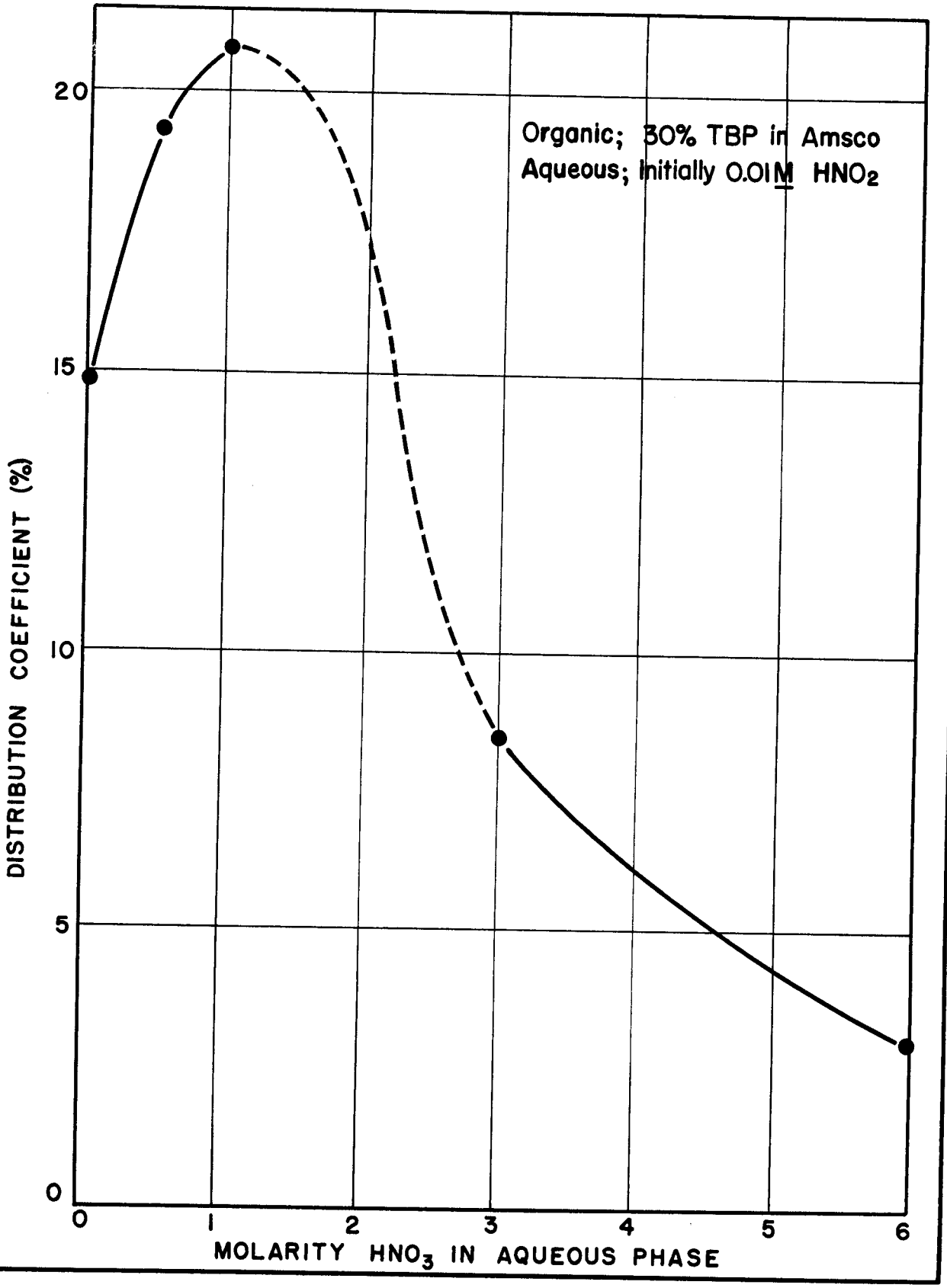

10.2 Stripping of Nitrous Acid from the Solvent

Data presented in Table 10.4 show the progress of extracting HNO_2 from TBP with 1 M HNO_3. The purpose here was to strengthen the reliability of the distribution coefficients obtained by showing the amount of nitrous acid that actually went into the organic. The extractions were slow and difficult as might be expected from the unfavorable distribution coefficient with respect to stripping. Additional stripping would probably have removed several more percent from the organic. Gas evolution was observed when the washed TBP was shaken with a solution of sulfamic acid, indicating the presence of residual nitrous acid.

Table 10.4

Nitrous Acid Stripping from TBP with 1 M Nitric Acid

Solvent: 35 ml of TBP containing Ca. 50 mg of HNO_2

Strip: 100 ml portions of 1 M HNO_3

Sample	No. of Washes	% of HNO_2 Stripped
1	3	16.2
2	5	22.2
3	4	16.7
4	4	14.3
5	4	6.9
6	4	4.0
Total	24	78.3

Exhaustive stripping of nitrous acid from 30% TBP in Amsco under the same conditions gave similar results; 27 washes were required to effect 90% removal of HNO_2.

11.0 Fumeless Dissolving (L. E. Line, Jr.)

A method[1] of N_2O_4 analysis of dissolver off-gases has been proposed which involves adsorption of nitrogen tetroxide in caustic and colorimetric nitrite determination with Greiss reagent. Study of the adsorption step was continued to establish the analytical accuracy of the method and to determine whether other nitrogen oxides might be produced in the reaction.

Other work was concerned with the feasibility of means proposed[19] for removing last traces of NO and N_2O_4 from the off-gas stream.

11.1 Material Balance of the Reaction Between N_2O_4 and NaOH

Since under some conditions, N_2O_4 may not react according to the equation:

$$N_2O_4 + 2\ NaOH \longrightarrow NaNO_3 + NaNO_2 + H_2O$$

without side reactions,[20,21] accurately known quantities of the gas were absorbed in 4 M NaOH and the results compared with those expected. The N_2O_4 was generated by careful decomposition of reagent grade $Pb(NO_3)_2$ in a stream of O_2 (to oxidize any NO that may have formed). A blank run with O_2 showed no change in nitrite concentration of a 150 ppm sodium nitrite solution. Table 11.1 shows that the amount of nitrite found was equal to that expected within 2 to 4%.

Table 11.1

N_2O_4 Generated by Decomposition of $Pb(NO_3)_2$

Sample	$Pb(NO_3)_2$	$NaNO_2$, g (expected)	$NaNO_2$, g (found)	% Difference
1	0.3989	0.0833	0.0812	2.4
2	0.2002	0.0417	0.0435	4.1

The following experiment indicates that very little NO, if any, is formed when N_2O_4 is absorbed in NaOH. Approximately 4 g of tank N_2O_4 was passed slowly (100-200 cc/min) through 4 scrubbers (fritted disk type) containing 4 M NaOH and the effluent passed into a fifth scrubber containing 100 ml of a saturated solution of $FeSO_4$ acidified with H_2SO_4. Thereafter the system was purged with N_2 in order to drive over any NO that might have become dissolved in the alkali. The characteristic dirty-green color due to $FeSO_4$. NO, sensitive to 1 part in 10,000, did not appear.

11.2 Scrubbing of N_2O_4 with KOH

In connection with studies of the thermal decomposition of N_2O conducted by the Unit Operations Section, a slight amount of N_2O_4 was observed in the effluent from the decomposition tube. Samples of this gas before and after scrubbing in a caustic tower were made available for colorimetric nitrite analysis (see Table 11.2). The stainless steel caustic scrubbing tower, about 1-1/4 in. in diameter and 30 in. long, was filled with a packing of short pieces of stainless steel tubing. Effluent gas from the thermal decomposition unit was passed through the tower at a velocity of about 1000 cc/min. countercurrent to a slow moving stream of approximately 20% KOH.

Table 11.2

Scrubbing of N_2O_4 by 20% KOH

Sample	Vol. % N_2O_4 in Gas Before Scrubbing	Vol. % N_2O_4 in Gas After Scrubbing
1	1.0	0.01
2	0.37	0.0037
3	0.11	0.042

The effluent gas (after scrubbing) was in each case colorless. Color in the influent of sample #3 containing only 0.1% was visible against a white background in a 300 ml sample tube.

Samples #1 and #2 show a high scrubbing efficiency but that of #3 is low. No explanation is offered to account for this.

11.3 Scrubbing of NO with HNO_3

Only preliminary work has been done to determine the efficiency of removal of NO by 70% HNO_3. It was found that when a stream of N_2 containing 1-2% NO was slowly led through five gas washers containing 70% HNO_3, copious brown fumes were released, presumably according to the equation:

$$2\ HNO_3 + NO \rightleftarrows 3\ NO_2 + H_2O$$

The conversion of NO to NO_2, if complete, would be satisfactory since the alkaline scrub would easily remove the NO_2. Under the conditions used, the above reaction was not complete. However, further studies are to be carried out in a packed column in countercurrent fashion.

12.0 The ORNL "mini" Mixer-Settler (V. A. Ryan)

The purpose of the ORNL mixer-settler is to facilitate the performance of countercurrent extractions which cannot be safely done in a hood using batch techniques. This unit is designed to operate in a hot cell, behind lead shielding. Mirrors will be used for observation, and simple remote control devices will make weir adjustments and obtain end stream and stage samples.

Details of the unit are given in previous reports. Briefly, it is a 20-stage, gear driven unit having mixing sections 1/2" wide x 1/2" long x 1-1/2" high and settling sections 1/2" wide x 1-1/4" long x 1-1/2" high (Fig. 12.1). Figure 12.2 shows the feed and scrub delivery system consisting of gear driven hypodermic syringes using mineral oil as displacement fluid. The solvent is fed directly with a Milton Roy "Mini" pump.

Using the mixer-settler under the Purex Flowsheet #1 operating conditions for 1A extraction, three runs have been completed. These are numbered 15a, 15b, and 16. Number 15b was most nearly satisfactory and is discussed here in full. The data obtained in Runs 15a and 16 will be found in Appendix F.

After 12 hours operation (Run 15a), stage samples were taken and the machine shut off for 12 hours. Then, operation was resumed for six hours (Run 15b). Stage samples were withdrawn which were analyzed and the data plotted to yield an equilibrium (x, y) diagram (Figure 12.3). Thus the run was not actually a six hour run but a resumed run of 18 hours total duration. The withdrawal of stage samples at the end of run 15a and the subsequent shutdown both disturb the steady state conditions obtained during run 15a.

In Figure 12.3, the squared points show sample data after an uninterrupted run of six hours. If the last stage is ignored as probably of low efficiency because of persistent flooding, about four and one-fourth theoretical stages were obtained in five actual stages, or 85% overall efficiency[22]. If stage efficiencies are calculated as the actual enrichment divided by the theoretical enrichment, the results for several stages are as follows:

Stage	Efficiency (%)
14	98
15	77
16	100
17	52
18	120
19	7.9
Average	76

Average omitting stage 19, 90%

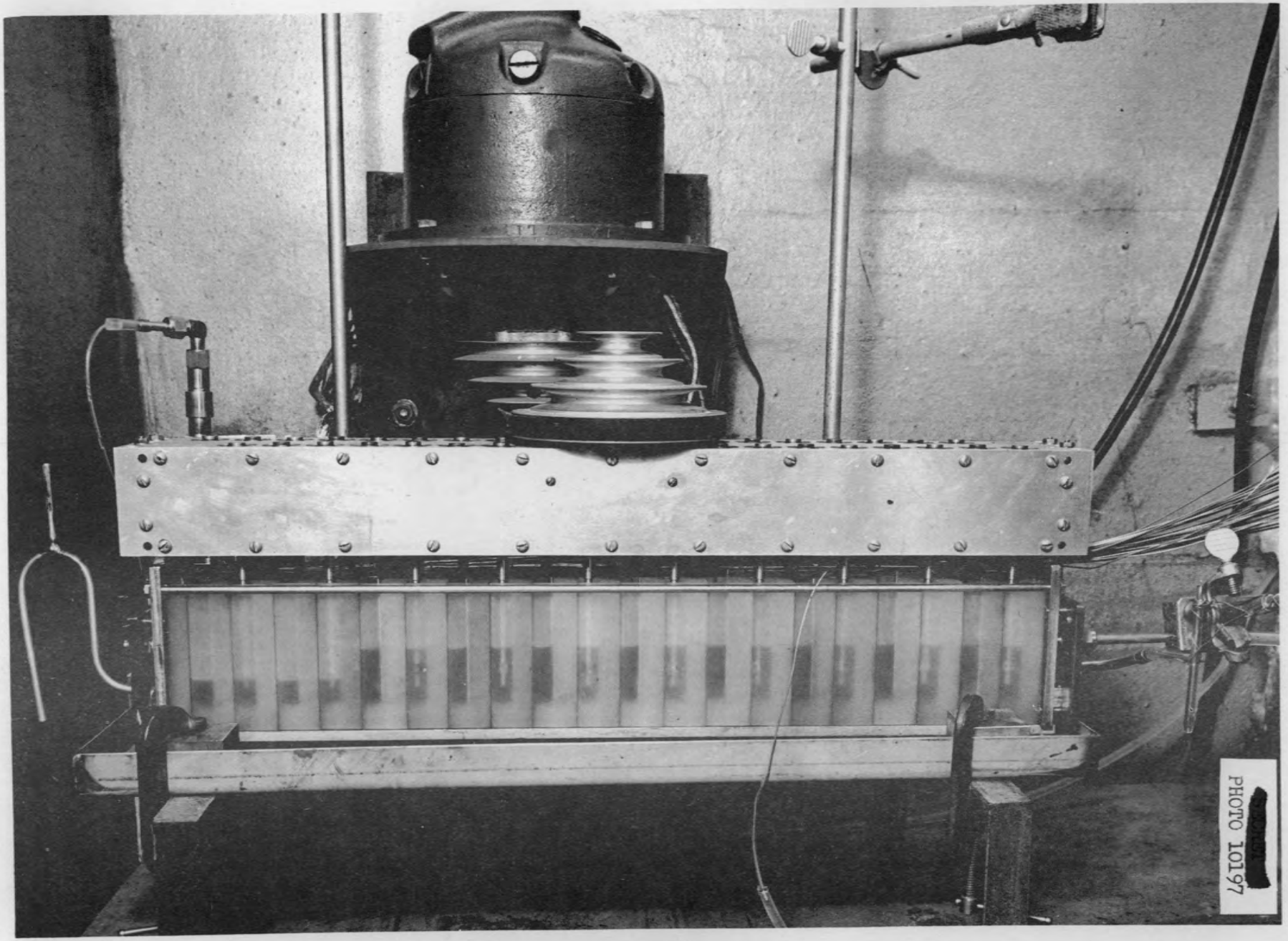

Figure 12.1
The ORNL "mini" Mixer-Settler

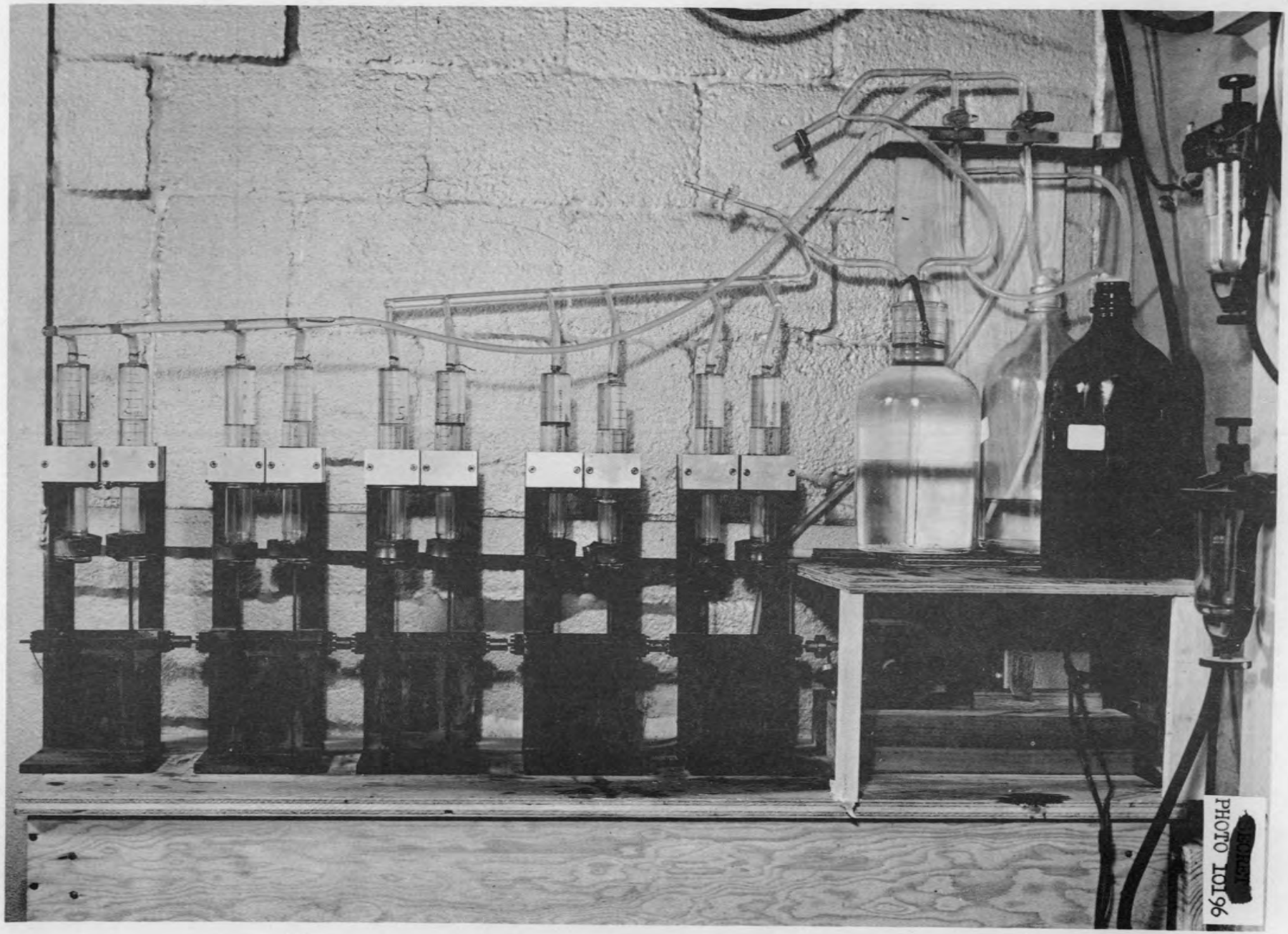

Figure 12.2

Mixer-Settler Feed Assembly

FIG. 12.3
STAGE DATA FOR URANIUM EXTRACTION—
PUREX IA OPERATION

[redacted]
Dwg. #15121

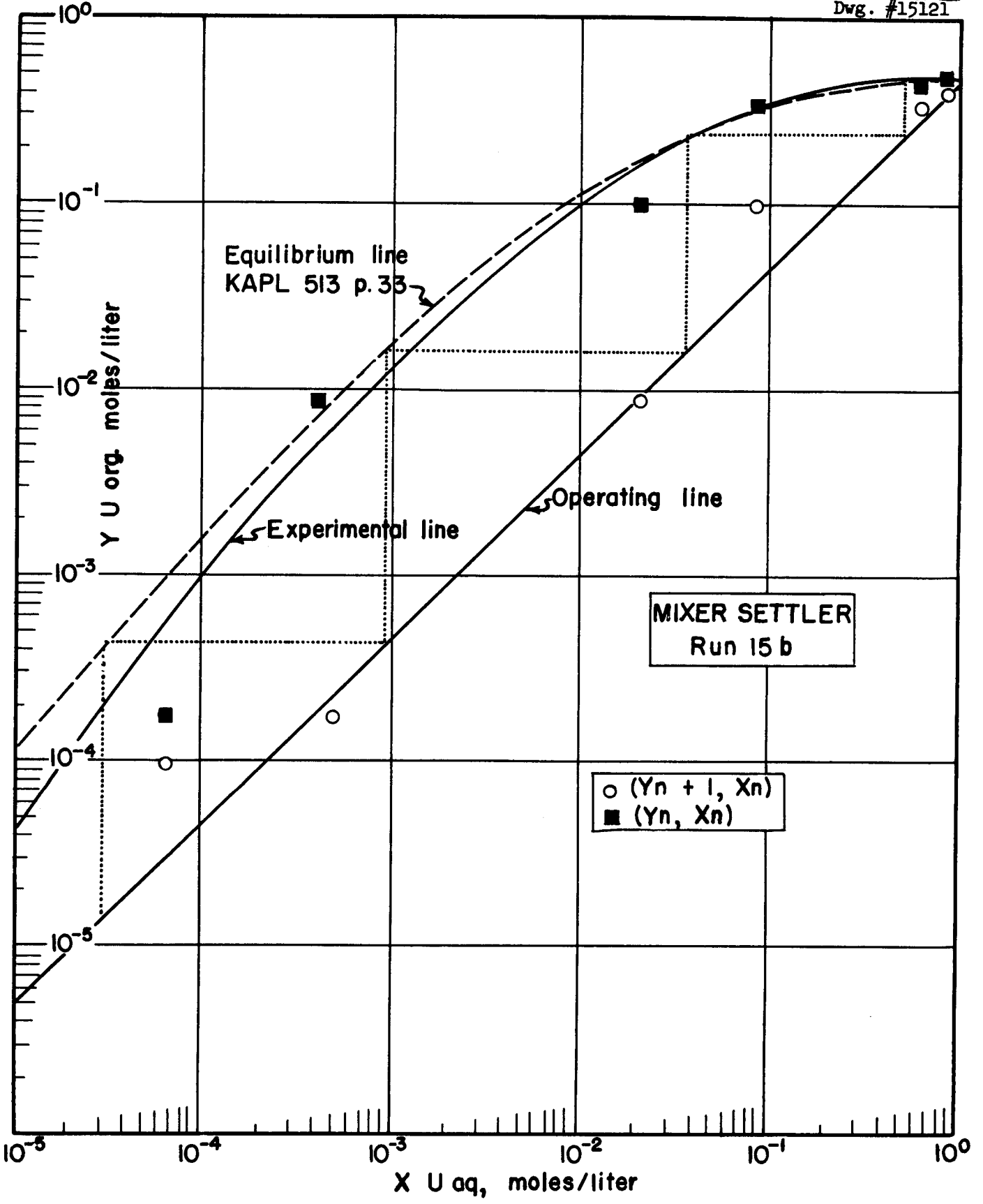

Qualitatively, the best-fitting curve (solid) lies within experimental error of the accepted (dotted) curve , except at the 19th stage. This can be taken to mean that the efficiency is within experimental error of 100%.

Uranium losses were about 0.002%.

The problem remains to secure operation that is trouble free and safe. Almost all of the mechanical difficulties initially encountered have been corrected. The fluorothene block continues to leak in spite of all efforts to prevent it from doing so. It is hoped that a tight block can be obtained by refabricating some of the parts according to a method described in KAPL-602. The new parts will be routed from 1" stock rather than sawed from 1/2" stock. In this way it is possible to eliminate the side sheets and their clamps and screws.

Further test runs will be made with the machine operated as a 16-stage unit by closing the aqueous port between stage four and five. The organic end stream will be withdrawn from stage four using a bellows pump, and the scrub will be admitted to stage five.

13.0 Bibliography

1. Line, L. E., Jr., Quarterly Report, CF memo 52-2-72, February 12, 1952.

2. Flanary, J. R., Stability of Purex Solvent in the Presence of 6 M HNO_3, CF memo 52-1-90, January 10, 1952.

3. Reilly, V. J., Quarterly Report: Miscellaneous Studies, CF memo 52-2-53, February 11, 1952.

4. Flanary, J. R., V. J. Reilly and F. R. Bruce, A Tail End Treatment for the Purex Process Uranium Product, CF memo 51-11-173, November 30, 1951.

5. Reilly, V. J., Quarterly Report, CF memo 52-2-79, February 13, 1952

6. Sheldon, E. B. and R. L. Folger, Tentative Plutonium Recovery Flowsheet, CF memo 51-11-90, November 19,1951.

7. Folger, R. L., Plutonium Recovery from Metallurgical Wastes: Dissolver Studies - Summary of Work on Synthetic (Non-Active) Materials, CF memo 51-8-236, August 29, 1951.

8. Folger, R. L., Quarterly Report, CF memo 51-11-54, November 12, 1951.

9. Folger, R. L. and S. V. Castner, Quarterly Report, CF memo 52-2-129, February 8, 1952.

10. Folger, R. L., E. B. Sheldon, and S. V. Castner, Quarterly Report, CF memo 52-2-173, February 10, 1952.

11. Sheldon, E. B., Quarterly Report, CF memo 52-2-208, February 14, 1952.

12. Sheldon, E. B. and R. L. Folger, Trip Report on Visit to Los Alamos and Hanford, CF memo 51-11-22, November 2, 1951.

13. Willard, H. H. and O. B. Winter, Volumetric Method for Determination of Fluoride, Ind. Eng. Chem., Anal. Ed., 5, 7 (1933).

14. Lanham, W. B. and J. R. Flanary, Purex Process Flowsheet No. 3, CF memo 51-9-103, September 19, 1951.

15. Hanford Progress Report, Chemical Development Section, HW-22566, September, 1951.

16. Gilbert, E. R., Mixer Settler Design for Recovery Area, DPK-128.

17. Riebsomer, J. L., Chem. Rev., 36, 196 (1945); Michael and Carlson, J. Am. Chem. Soc. 57, 1268 (1935); ibid 59, 843 (1937); J. Org. Chem. 4, 169 (1939).

18. Yost, D. M. and H. Russell, Jr., Systematic Inorganic Chemistry, Prentice-Hall, New York, 1944, p. 80.

19. Gresky, A. T., Recovery of Nitrogen Oxides and Rare Gas Fission Products from the Nitric Acid Dissolution of Irradiated Uranium, ORNL-1208, March 25, 1952.

20. Burdick and Freed, J. Am. Chem. Soc. 43, 518 (1921).

21. Mellor, J. W., Comprehensive Treatise on Theoretical and Inorganic Chemistry, Vol. VIII, p. 539.

22. Tabor, B. L., and V. A. Ryan, Quarterly Report, CF memo 52-2-183, February 11, 1952.

14.0 Appendix

A. Analytical Details

All of the specific DF's were calculated from niobium and zirconium activities measured by scintillation counting. This is believed to be much more accurate than beta counting for niobium where the beta energy is so low that the counting efficiency at 10% geometry is only about 0.3%. The counting efficiency for niobium gamma in the 3550 building scintillation counter is 30%, so that a counting rate roughly 100 times higher is obtained by the latter method. Also, slight changes in the charcter of the precipitate or mounting conditions will have negligible effect in scintillation counting, in contrast with their large effect in beta counting. Zirconium was also counted by this method to keep the results on the same basis.

The scintillation counter was compared directly with the building 3550 ion chamber by counting aliquots of a solution of niobium tracer in both instruments. The ratio found for niobium is 5000 scintillation c/min/mv on the 10" scale. Since the gamma energy and percentage is nearly the same for zirconium as for niobium, this factor will also apply fairly well for zirconium.

The relationship between the ruthenium gamma reading in the ion chamber and its radiation in beta c/min was required to check the balance of activity obtained by radiochemical analysis against the gross γ reading. A sample of ruthenium tracer was obtained by denitration of the run 13 effluent, wherein much of the ruthenium distilled and was collected in water. This solution was measured on the ion chamber and beta counted. The ratio was found for the fresh solution to be 1340 beta c/min/mv on the 10" scale, building 3550 ionization chamber. A portion of this ruthenium tracer was retained and measured periodically on the ion chamber to keep the ruthenium correction up-to-date. Generally, agreement between the gross gamma calculated from radiochemical analyses and that actually found, was rather good; - 0.6 to + 0.4 mv/ml was unaccounted for with total activities between 5 and 35 mv/ml.

Niobium decay had to be taken into account as some of the runs necessarily extended over rather long periods (up to 10 days). This effect was minimized in Runs SG-15, 16, and 17 by analyzing all the samples (including feeds) at the end of the run, rather than as they were collected. In Runs 12, 13, and 14, and in cases where recheck analyses were required, correction was made by assuming niobium would decay according to its half life. This is a fair assumption because of the small amount of zirconium in the samples in relation to the niobium.

B. Calculation of the Integral Decontamination Factor

A stepwise method was used for integrating Figures 5.61, 5.62, and 5.63 to obtain Figures 5.64 and 5.65 as the accuracy of the data did not warrant the use of the differential equation. The method depends on the following equations.

(1) Composite activity of effluent per unit volume $= \frac{A}{D_1}\Delta L_1 + \frac{A}{D_2}\Delta L_2 \cdots \quad \frac{1}{\Delta L_1 + \Delta L_2} \cdots$

Where A = activity in feed, per unit volume, a constant, and

ΔL_1, ΔL_2 ... = incremental volumes of effluent whose decontamination factors from feed are D_1, D_2, ...

Equation (1) may be rewritten as the composite unit activity of the effluent =

(2) $$A \left(\frac{\sum \frac{\Delta L}{D}}{\Delta L} \right)$$

(3) The integral DF = $$\frac{A}{A \left(\frac{\sum \Delta L / D}{\sum \Delta L} \right)}$$

(4) $$= \frac{\sum \Delta L}{\sum \frac{\Delta L}{D}}$$

The values of D, the instantaneous DF, were taken as the average over the increment. For example, the DF for niobium in Run 13 at 3 liters was 15. The previous and suceeding values are at 1 liter and 6 liters. The value of 15 was taken for all that solution collected between 2 and 4.5 liters.

True integration of equation (1) would lead to

$$\text{integral DF} = \frac{1}{\frac{1}{L}\int \frac{1}{D}\, dL}$$

The integral could be determined by plotting $\frac{1}{D}$ vs. L, and measuring the area under the curve.

C. Treatment of Residues from Slag and Crucible Recovery Dissolver

The residues from runs DG-1, DG-2, DG-3, and DG-4 have been dissolved singly by various means and the total weight of plutonium in each residue has been obtained. The combined residues from runs DG-5 and DG-6 have also been analyzed. The results are given in Table C-1.

The best method for treating the residues found thus far is as follows: The residues are boiled in 6 M HCl for approximately five minutes and the slurry is filtered. This removes between 95% and 99+% of the plutonium. The remainder of the residue, which is mostly silica, is then dissolved in concentrated hydrofluoric acid. There is still a small amount of a black powdery residue which is difficultly soluble in boiling 6 M HCl. This material, thought to be chromous oxide, contains less than one-tenth percent of the initial plutonium.

Table C-1

Plutonium Losses to Dissolver Residues

Run No.	Dissolver Residue (g)			Plutonium Assay (mg)			
	Initial Weight	After HCl Wash	After HF Wash	HCl Wash	HF Wash	Final* Wash	Total
DG 1	16.5						37.4
2	23.8						14.2
3	18.3	4.3	0.1	274	22	0.05	296
4	20	5	0.1	47.2	40.2	0.05	87.4
5,6	43.8	7.4	0.1	35	3.1	0.07	38.1

* The reagents were varied from run to run (HF, HCl, H_2SO_3, etc.) in attempts to obtain complete dissolution.

D. Calculation of Feed Composition (Ref. 12)

Solution	Volume (liters)	Ca(2)		Mg(3)		Al(4)	
		Moles	M	Moles	M	Moles	M
DG-1	19(1)	3.67	0.19	15.0	0.79	6.10	0.32
DG-2	20	4.10	0.21	17.2	0.86	6.59	0.33
DG-3	18.5	4.10	0.22	21.1	1.14	6.59	0.36
DG-4	16.9	4.10	0.24	15.9	0.94	6.59	0.39
DG-5	18.8	4.10	0.22	20.7	1.10	6.59	0.35
DG-6	20.0	4.10	0.21	16.4	0.82	6.59	0.33

(1) 17 liters DG-1 diluted with 1.9 liters 1 M ANN solution

(2) Assuming Ca (metal) 1.05 moles

CaF_2 2.65 "

CaI_2 0.40 "

(3) MgO in crucible 11.4 moles

MgO "sand"	DG-1	DG-2	DG-3	DG-4	DG-5	DG-6
Moles Mg	5.3	5.8	9.7	4.5	9.3	5.0

(4) Al gasket 0.19 moles

ANN added DG-1 4.5 m in dissolution + 1.9 m adjustment

DG-2 to 6 6.4 moles

E. Determination of Nitrous Acid Distribution Coefficients - Method and Calculations

The distribution coefficient of nitrous acid between organic and aqueous phases was determined in the following manner. Fifty milliliters of aqueous HNO_3 of the requisite strength was added slowly at 0°C to 50 ml of 0.02 M $NaNO_2$. After mixing, a 10-ml aliquot was withdrawn for analysis. The remaining 90 ml was transferred to a 125-ml separatory funnel together with 35 ml of organic solvent.

The free space (10 ml) was swept with N_2 to remove O_2 and the mixture stoppered and shaken vigorously. After shaking, the aqueous phase was cooled to 0°C and a 10-ml aliquot withdrawn for analysis. Analyses were made colorimetrically[1] of solutions that had been diluted 1000-fold; they contained 10% by volume of the colorimetric reagent.

Since the colored solutions conform essentially to Beer's Law[1], it follows that the concentration of nitrite is directly proportional to the optical density $D = -\log I/Io$, wherein I/Io is the fraction of the light transmitted. The distribution coefficient may be calculated from the expression:

$$DC(org/aq) = \frac{D_1 - D_2}{D_2} \times \frac{90}{35}\ ^*$$

wherein D_1 and D_2 are the optical densities of samples of the aqueous phase before and after extraction, respectively.

The stripping experiments were carried out immediately after extraction. One-hundred milliliter portions were added to the organic in the 125-ml separatory funnel and the contents shaken vigorously, analyses being performed on the cumulative extracts after each third or fourth extraction.

* The factor 90/35 must be included because the concentration in the organic phase is 90/35 times the decrease in the concentration of the aqueous phase, $D_1 - D_2$.

F. Mixer-Settler Run Data-Purex 1A Operation

Conditions:

AF: 1.35 M uranium - 2 M HNO_3

AX: 30% TBP in Amsco

AS: 3 M HNO_3

Flow Ratio: AF/AX/AS = 1.42/4.75/.92 ml/min

Run 15a

Product and waste samples were taken at one hour intervals. End Stream samples.

	Solvent Product		Aqueous Wastes	
Hours from Startup	Uranium (g/l)	HNO_3 (M)	Uranium (g/l)	HNO_3 (M)
1	98.8	0.17	0.032	2.45
2	100.2	0.17	0.011	1.95
3	97.0	0.17	0.008	2.98
4	98.8	0.16	0.011	2.42
5	100.2	0.15	0.009	2.35
6	97.0	0.15	0.013	2.37
7	99.6	0.15	0.009	2.40
8	100.2	0.15	0.009	2.30
9	97.0	0.15	0.017	2.40
10	100.2	0.15	0.012	2.28
11	100.2	0.14	0.010	2.28
12	97.0	0.14	0.004	2.28

Extraction stage samples taken after 12 hours operation

14 (feed plate)	121.2	0.06	229.2	2.29
15	113.4	0.11	176.8	2.66
16	88.4	0.23	44.2	3.40
17	366.5	0.02	5.29	3.60
18	3.80	0.59	0.13	3.40
19	0.886	0.56	0.02	2.93
20	0.789	0.37	0.01	2.25

Run 15b

End stream samples

Hours from Startup	Solvent Product Uranium (g/l)	Solvent Product HNO_3 (M)	Aqueous Waste Uranium (g/l)	Aqueous Waste HNO_3 (M)
13	96.4	0.16	0.009	2.00
14	98.4	0.14	0.020	2.20
15	100.0	0.15	0.003	2.40
16	98.4	0.15	0.005	2.40
17	98.4	0.14	0.004	2.40
18	98.4	0.15	0.004	2.40

Extraction Stage Samples - taken after 18 hours operation

14 (feed plate)	115.0	0.07	202.5	2.43
15	106.0	0.14	143.75	2.70
16	82.4	0.28	19.4	3.67
17	24.5	0.61	4.98	3.75
18	2.100	0.71	0.095	3.60
19	0.042	0.62	0.015	3.10
20	0.023	0.48	0.002	2.25

Run 16

End Stream Samples

1	105	0.11	1.00	1.34
2	84.8	0.19	0.38	1.33
3	88.5	0.15	2.30	1.70
4	87.0	0.14	0.296	2.01
5	91.3	0.14	0.008	2.47
6	85.5	0.15	0.03	2.56
7	87.5	0.14	0.531	2.44
8	84.8	0.14	0.008	2.62
9	81.5	0.14	0.026	2.68
10	83.3	0.14	0.017	2.43

Extraction Stage Samples - taken after 10 hours operation

14 (feed plate)	95.0	0.12	258.0	2.30
15	103.0	0.06	207.0	2.45
16	102.5	0.09	186.0	2.75
17	47.3	0.19	52.3	3.36
18	49.3	0.44	0.177	0.26
19	39.5	0.49	3.70	3.29
20	--		0.025	2.07